NATIONAL ADVISORY COMMITTEE FOR AERONAUTICS

REPORT 1219

MEASUREMENT AND ANALYSIS OF WING AND TAIL BUFFETING LOADS ON A FIGHTER AIRPLANE

By WILBER B. HUSTON and T. H. SKOPINSKI

1955

For sale by the Superintendent of Documents, U. S. Government Printing Office, Washington 25, D. C. Yearly subscription, $10: foreign, $11.25: single copy price varies according to size. - - - - - - - - - Price 30 cents

REPORT 1219

MEASUREMENT AND ANALYSIS OF WING AND TAIL BUFFETING LOADS ON A FIGHTER AIRPLANE

By WILBER B. HUSTON and T. H. SKOPINSKI

Langley Aeronautical Laboratory
Langley Field, Va.

National Advisory Committee for Aeronautics

Headquarters, 1512 H Street NW., Washington 25, D. C.

Created by act of Congress approved March 3, 1915, for the supervision and direction of the scientific study of the problems of flight (U. S. Code, title 50, sec. 151). Its membership was increased from 12 to 15 by act approved March 2, 1929, and to 17 by act approved May 25, 1948. The members are appointed by the President, and serve as such without compensation.

REPORT 1219

MEASUREMENT AND ANALYSIS OF WING AND TAIL BUFFETING LOADS ON A FIGHTER AIRPLANE [1]

By Wilber B. Huston and T. H. Skopinski

SUMMARY

The buffeting loads measured on the wing and tail of a fighter airplane during 194 maneuvers are given in tabular form, along with the associated flight conditions. Measurements were made at altitudes of 30,000 to 10,000 feet and at speeds up to a Mach number of 0.8. Least-squares methods have been used for a preliminary analysis of the data.

In the stall regime, the square root of the dynamic pressure was found to be a better measure of the load than was the first power. The loads measured in maneuvers of longer duration were, on the average, larger than those measured in maneuvers of short duration. Considerable load alleviation was obtained by a gradual entry into the stall. In the shock regime, the magnitude of the load at a given speed and altitude was determined by the extent of the penetration beyond the buffet boundary. For a modification of the basic airplane in which the wing natural frequency in fundamental bending was reduced from 11.7 to 9.3 cps by the addition of internal weights near the wing tip, a 15-percent decrease in wing loads and a similar percentage increase in tail loads resulted.

The loads on a simplified wing buffeting model are examined on the assumption that buffeting is the linear response of an aerodynamically damped elastic system to an aerodynamic excitation which is a stationary random process. The agreement between the results of this analysis and the loads measured in stalls is sufficiently good to suggest the examination of the buffeting of other airplanes on the same basis.

INTRODUCTION

An early investigation of buffeting which utilized the North American F–51D airplane (ref. 1) provided basic information on the flight conditions under which buffeting was encountered and provided measurements of the magnitude of the buffeting loads on the horizontal tail. Speed and altitude were shown to be primary variables, and the load data were reduced to dimensionless coefficient form by means of the product: Dynamic pressure×Tail area. It was hoped that such a buffeting-load coefficient might be applicable to other airplanes, but the assumption that a form of coefficient common in steady-state aerodynamics would be applicable to a dynamic phenomenon was recognized as requiring further investigation.

Since the completion of the tests of reference 1, a number of other experimental flight and wind-tunnel studies have been conducted. The effects of airfoil section and plan form on buffeting have been investigated. Buffet boundaries of a number of specific airplanes have been obtained. In several instances wing and tail loads have been measured during buffeting with special research airplanes. An analytical approach has also been made to the buffeting-loads problem, based on methods developed in the study of stationary random processes (see ref 2).

Upon completion of the tests of reference 1, plans were made to extend these tests of the same airplane to measure wing loads and tail loads simultaneously during buffeting and, at the same time, to measure the effect of maneuver rate and the effect of penetration beyond the buffet boundary. In addition, the altitude coverage was to be improved in order to resolve more clearly the effect of this variable and, since it was thought that structural frequency might also be a significant variable, provision was made to modify the wings for several tests in order to measure some buffeting loads with a reduced wing frequency.

The purpose of the present report is to present the results of these extended flight tests and, especially, to present the magnitude of the buffeting loads measured. The basic load data involving 194 runs are given in tabular form, together with associated flight conditions. The results of preliminary studies which illustrate certain trends in the data are also given, but this analysis is not intended to be definitive. Although the present tests do not cover either the configurations or the speed range of greatest current interest, some of the variables are covered more extensively than in other tests. Stall buffeting, in particular, which will probably be common to all airplanes whatever the configuration, is extensively covered, and it is believed that all the data may be of value to those who are interested in the prediction of buffeting loads. The results of an analytical study in which the methods of generalized harmonic analysis are applied to a simplified wing buffeting model are given in an appendix.

SYMBOLS

A	aspect ratio, $b/\bar{c}$
A, B	constants used in tail-load equations
a, b	constants used in wing-load equations
b	wing span, ft
$(C_{L_\alpha})_{eff}$	effective slope of lift curve for damping of small oscillations of a stalled wing in first bending mode
C_N	airplane normal-force coefficient, nW/qS
$\overline{c_n{}^2}$	mean-square value of coefficient of section-normal-force fluctuations in buffeting
$\bar{c}$	average wing chord, S/b
f	frequency, cps
h_p	pressure altitude, ft
k	wing stiffness, lb/ft

[1] Supersedes NACA TN 3080, 1954.

L	root structural shear load due to buffeting, lb
ΔL	amplitude of maximum root-structural-shear fluctuation due to buffeting encountered during run, lb
M	Mach number
n	normal load factor
P	penetration beyond buffet boundary (defined in eq. (13))
q	dynamic pressure, lb/sq ft
r	coefficient of linear correlation
S	area, sq ft
s	standard error
t	time, sec
Δt_{load}	time between onset of buffeting and occurrence of measured load ΔL
V	true airspeed, ft/sec
W	airplane weight, lb
α	angle of attack, radians
ω	circular frequency, $2\pi f$, radians/sec
ϵ	residual, that is, a measured value minus a calculated value

Subscripts:

av	average over class
B	onset of buffeting
BB	buffet boundary
E	end of buffeting
L	left
max	maximum
n	natural
R	right
T	tail
W	wing

Mean values are designated by a bar (as $\overline{c_n{}^2}$); time differentiation by a dot (as $\dot{\alpha}$).

Note: Symbols used only in appendixes are defined where they occur.

AIRPLANE AND INSTRUMENTATION

AIRPLANE

The airplane used for the present tests was the same North American F–51D airplane with heavily reinforced horizontal tail, fuselage, and wing used for the investigations reported in references 1 and 3. The test airplane is shown as a three-view diagram in figure 1, and as a photograph in figure 2.

The airplane is equipped with a Packard V–1650–7, 12-cylinder engine and a 4-bladed Hamilton Standard Hydromatic Propeller, 11 feet 2 inches in diameter. The propeller-to-engine gear ratio is 0.479 to 1. Geometrical data for the airplane are listed in table I. The natural structural frequencies of various components as determined by ground vibration tests are listed in table II. In this table two sets of values of wing natural frequency are shown. One set applies to the basic airplane configuration and to the greater portion of the tests reported herein; the other set applies to the modified airplane, that is, the airplane with 100-pound weights added internally near the wing tips in order to lower the wing natural frequency in the fundamental bending mode from 11.7 to 9.3 cps.

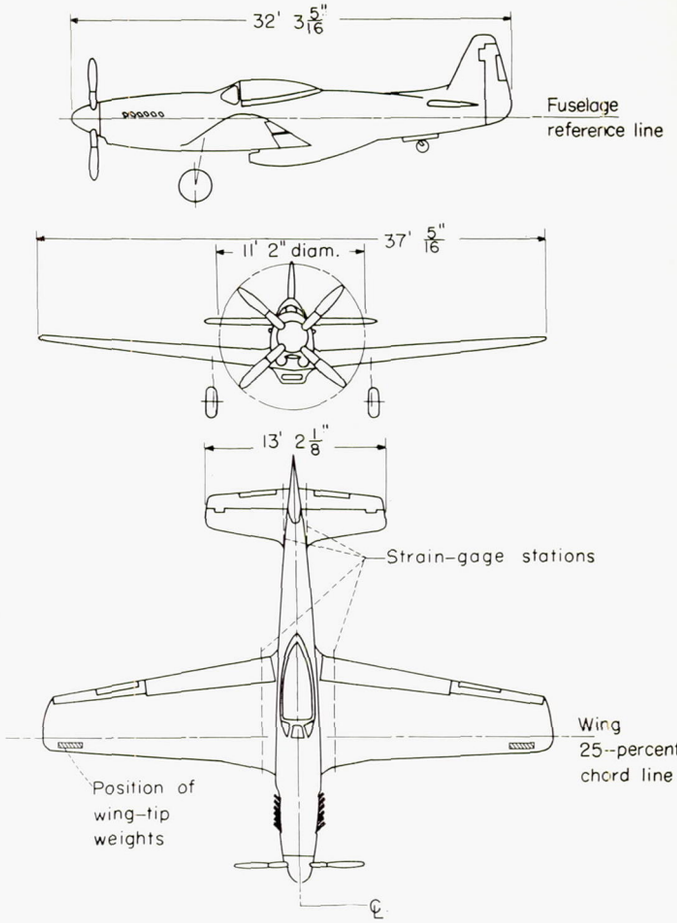

FIGURE 1.—Three-view diagram of test airplane.

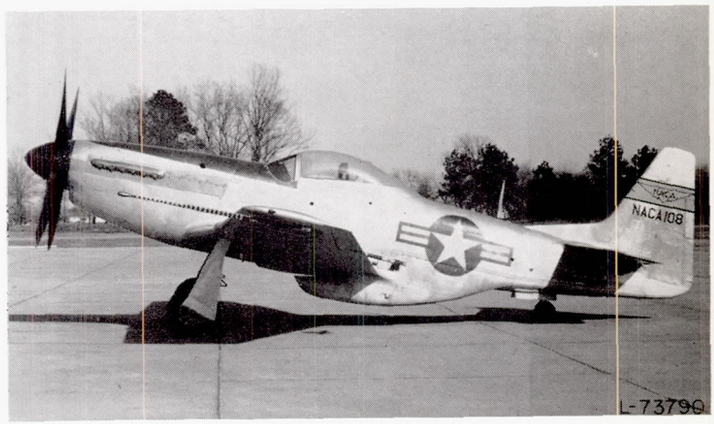

FIGURE 2.—Side view of test airplane.

TABLE I.—GEOMETRICAL DATA FOR TEST AIRPLANE

Wing:	
Span, ft	37. 03
Area, sq ft	240. 1
Mean aerodynamic chord, ft	6. 63
Aspect ratio	5. 71
Root thickness ratio	0. 15
Tip thickness ratio	0. 12
Taper ratio	0. 462
Horizontal tail:	
Span, ft	13. 18
Area, sq ft	41. 0

TABLE I.—GEOMETRICAL DATA FOR TEST AIRPLANE—Cont.

Weight at take-off, lb:	
Basic airplane	8, 995
Modified airplane	9, 149
Center-of-gravity position at take-off, percent M.A.C.:	
Basic airplane	27. 2
Modified airplane	25. 3

TABLE II.—NATURAL FREQUENCY OF AIRPLANE COMPONENTS

	Basic airplane	Modified airplane
Wing:		
Fundamental bending frequency, cps	11. 7	9. 3
First asymmetric bending frequency, cps	22. 3	18. 1
Torsion frequency, cps	38. 0	34. 5
Second symmetric bending frequency, cps	----	52. 0
Horizontal stabilizer:		
Primary bending frequency, cps	25. 0	25. 0
First asymmetric bending frequency, cps	36. 0	36. 0
Torsion frequency, cps	70. 0	70. 0
Fuselage:		
Torsion frequency, cps	9. 8	9. 8
Side bending frequency, cps	12. 5	12. 5
Vertical bending frequency, cps	14. 9	14. 9

INSTRUMENTATION

Standard instruments.—Impact pressure, pressure altitude, and normal acceleration were measured as functions of time with standard NACA recording instruments. The airspeed head was mounted on a boom extending 1.2 chords ahead of the leading edge of the wing near its right tip, and the NACA airspeed-altitude recorder was located near the boom to minimize lag effects which are believed to be negligible for the rates of change of altitude or airspeed encountered. The airspeed system was calibrated for position error up to a Mach number of 0.78; this calibration made possible the determination of the flight Mach number to within ± 0.01.

Airplane normal force was measured with an accelerometer mounted near the airplane center of gravity. The sensitive element had a natural frequency of 16 cps and was air damped. The damping was adjusted to 0.6 of critical at sea level, except during the tests with the modified wing, when the damping was changed to 0.6 of critical at a pressure altitude of 30,000 feet.

Strain-gage installation.—Measurements of structural shear on the wing and horizontal tail were made by means of wire resistance strain gages wired in four-active-arm bridges and attached near the roots of the principal structural members. Shear bridges were attached to the spar webs and bending-moment bridges, to the spar flanges. The entire installation was calibrated by established methods. (See ref. 4.) For the shear on a wing panel, this calibration resulted in two combined strain-gage channels. One of these combined channels was principally sensitive to shear and secondarily sensitive to bending moment; the other channel was primarily a measure of bending moment and secondarily sensitive to shear. The outputs of these two channels, recorded as a function of time on a multiple-channel recording oscillograph, could be combined numerically to obtain the wing-panel structural shear. The shear on the left and right panels of the horizontal stabilizer was obtained from the outputs of the left and right combined strain-gage channels which were sensitive to shear. This strain-gage system represents an improvement over that used in reference 1.

The recording oscillographs used employed galvanometer elements with a natural frequency of 100 cps which were damped to about 0.6 of critical damping. This combination of damping and natural frequency insured an approximately linear response for the buffeting frequencies expected. Special care was taken to balance the galvanometer elements so as to keep any possible acceleration effects within the reading accuracy. Variations in sensitivity due to voltage changes were eliminated by provision of a calibrate signal on the record for each run, and the stability of the strain-gage installation was checked at intervals by application of known loads to the wing and tail. The overall experimental error in incremental values of wing root shear obtained from the strain-gage—oscillograph system is estimated from the calibration as less than ± 130 pounds; whereas for the incremental values of shear on the right and left horizontal stabilizer the estimated error is of the order of ± 80 pounds.

TESTS

All tests were made with the airplane in the clean configuration, and the power setting, at low Mach numbers, was that required to attain level flight at the altitude of test. In tests at Mach numbers greater than the level-flight capabilities of the airplane, normal rated power was used. Of a total of 194 runs in which buffeting was measured, 150 were made with the basic airplane and 44 with the modified airplane.

With the basic airplane, gradual turns to the stall were performed at nominal test altitudes of 30,000, 25,000, 20,000, 15,000, and 10,000 feet. Pull-ups were performed at 30,000, 25,000, and 20,000 feet. The range of Mach numbers covered was 0.34 to 0.792 at 30,000 feet and 0.23 to 0.41 at 10,000 feet.

With the modified airplane, the added wing-tip weights introduced local stress concentrations which restricted the maximum allowable load factor for buffeting flight to 4 and limited the maneuvers to pull-ups. With the airplane at 30,000 feet, buffeting cannot be obtained at speeds between $M=0.54$ and $M=0.73$, without exceeding the limit load factor of 4; whereas at 10,000 feet, buffeting is not encountered at speeds between $M=0.32$ and the maximum permissible diving speed which for the standard North American F–51D airplane is a true airspeed of 537 mph. For the modified airplane, buffeting was, therefore, obtained by performing pull-up maneuvers at 30,000 feet and 10,000 feet at speeds limited by the foregoing considerations.

METHOD OF OBTAINING DATA

The procedure and definitions used in presenting the results of this investigation are best illustrated by referring to the typical time-history records shown in figure 3. The accelerometer record (fig. 3(a)) was used to establish the time for the beginning t_B and end t_E of buffeting, as well as the duration of buffeting. These values were obtained simply by observing the point at which there was a distinct change in the character of the accelerometer trace. The airplane normal-force coefficient C_N was obtained from the accelerometer and airspeed records. Values of C_N during buffeting

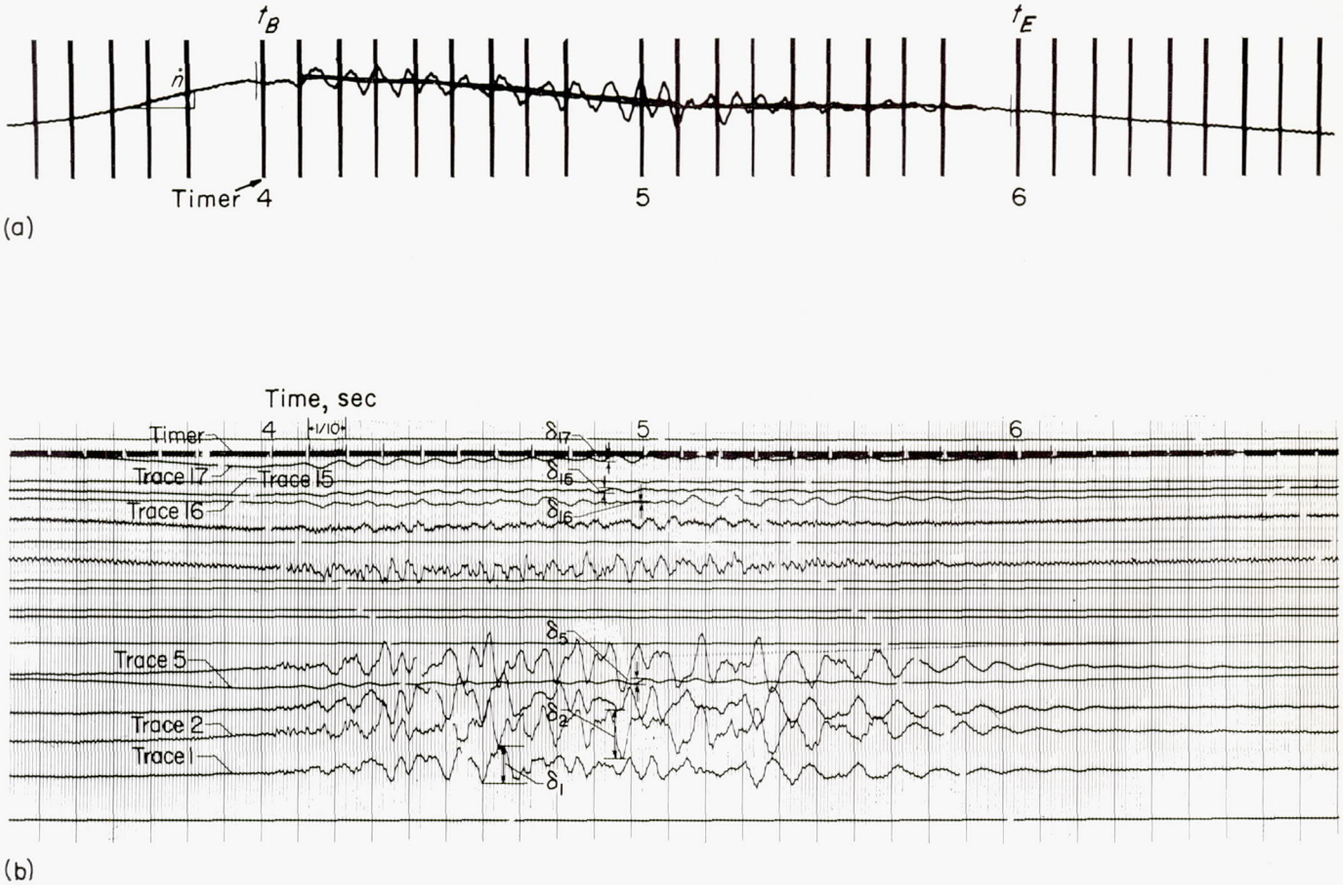

(a) Accelerometer record illustrating times selected for start and end of buffeting.
(b) Oscillograph record showing data selected for buffet load evaluation.

FIGURE 3.—Typical flight buffeting records.

were based on a mean line faired through the fluctuations of the accelerometer record. The airplane normal-force coefficients at the beginning C_{N_B} and end C_{N_E} of buffeting were determined and corresponding values of Mach numbers M_B and M_E were also noted. In determining all values of airplane normal-force coefficient, the value of airplane weight W used for each run was the take-off weight corrected for the fuel consumed prior to the start of the run. The maximum rate of change of airplane normal load factor $\dot{n}$ prior to the onset of buffeting was determined for each run, as in figure 3 (a), and the maximum rate of change of angle of attack per chord traveled $\dot{\alpha}\bar{c}/V$ was estimated from $\dot{n}$ on the assumption that the speed remains constant and

$$\dot{\alpha}=\frac{dC_N/dt}{dC_N/d\alpha}=\frac{\dot{n}W}{qS\,(dC_N/d\alpha)}$$

and hence that

$$\frac{\dot{\alpha}\bar{c}}{V}\approx\frac{\dot{n}}{n_B}\frac{C_{N_B}}{dC_N/d\alpha}\frac{c}{V}$$

In this relation, a nominal value of 5.3 was used for $dC_N/d\alpha$.

A typical oscillograph record for obtaining wing and tail loads is shown in figure 3 (b). The six traces identified with numbers in this figure were employed. Traces 1 and 2 are measures of root shear on the right and left horizontal tail, respectively. Root shear on the left wing panel is measured by a combination of the deflections of traces 15 and 17 and on the right wing, by a combination of traces 5 and 16. Buffeting loads, which are incremental loads, were determined from the peak-to-peak deflections of these traces (designated δ_1, etc., in fig. 3 (b)). The buffet-load values ΔL reported for a run are one-half of the largest peak-to-peak fluctuation in each of the four loads encountered during that run. The time of each load maximum was recorded and is reported as the incremental time Δt_{load} following the onset of buffeting. Through use of a timer common to the standard flight instruments, values of M, C_N, and q corresponding to each buffeting load were determined.

RESULTS

BUFFET BOUNDARY

The data acquired in the present investigation of the basic airplane are incorporated in table III. For the modified airplane the data are included in table IV. Tables III (a) and IV (a) deal with the operating conditions under which buffeting was first encountered and under which it ended. In addition to the numerical data, a pilot's note column is included. In most instances the pilot estimated the intensity of buffeting in one of four categories: very light, light, moderate, or heavy. These comments have been designated by the letters vl, l, m, and h. The pilot's notes on the direction of the roll-off after the stall are also included, left and right roll being designated by L and R, respectively, while no roll is indicated by N.

TABLE III.—BUFFETING CONDITIONS AND LOADS OF BASIC AIRPLANE

(a) Operating Conditions

Run	M_B	C_{N_B}	h_p, ft	$\dot{n}$, g/sec	$\frac{\dot{\alpha}\bar{c}}{V}$	Δt, sec	M_E	C_{N_E}	Pilot's note (a)
Turns at an altitude of 30,000 ft									
1	0.337	1.220	29,200	0.60	1.67×10^{-3}	3.62	0.321	0.881	l
2	.341	1.145	30,730	.15	.44	2.60	------	------	--------
3	.347	1.208	30,000	.55	1.46	5.18	.327	.935	--------
4	.357	1.125	30,300	0	0	2.30	------	------	l
5	.365	1.147	30,600	.40	.94	------	------	------	--------
6	.367	1.150	29,800	.55	1.20	.80	.366	1.087	vl
7	.368	1.105	30,100	.40	.88	5.30	--------	------	l
8	.370	1.130	30,700	.50	1.14	2.60	------	------	l
9	.404	1.150	29,900	1.00	1.68	3.10	.370	.810	l
10	.413	1.100	30,900	.36	.59	1.40	.394	.875	l
11	.460	1.099	30,500	1.60	1.86	1.58	.434	.798	m
12	.484	1.070	30,500	.61	.60	1.38	.461	.945	m
13	.499	1.050	29,700	2.1	1.84	------	------	------	m
14	.510	1.048	30,500	.90	.76	1.30	------	------	m
15	.514	1.088	30,900	3.30	2.80	1.50	------	------	m
16	.530	1.105	31,500	3.20	2.52	1.28	.511	.960	m
17	.542	1.083	31,000	1.00	.73	1.40	.525	.980	l
18	.586	------	31,900	------	----------	1.1	.586	------	m
19	.595	1.095	30,000	3.6	2.05	1.25	.577	.855	h, L
20	.607	1.066	29,500	1.30	.63	2.35	.605	.845	m
21	.610	1.098	29,700	1.10	.53	1.10	------	------	--------
22	.633	------	31,800	------	----------	.90	.625	------	m
23	.641	1.020	29,250	.40	.16	2.10	------	------	--------
24	.644	1.043	27,700	3.00	1.10	1.32	.640	.710	h
25	.649	.995	29,900	3.80	1.52	1.15	.625	.999	h, N
26	.687	------	30,400	------	----------	2.2	.695	------	--------
27	.692	------	30,000	------	----------	2.1	.671	------	h
28	.700	------	29,500	------	----------	2.35	.690	------	vl
29	.702	.721	27,830	------	----------	2.70	------	------	--------
30	.719	------	30,000	------	----------	------	------	------	m
31	.768	------	29,300	------	----------	------	------	------	--------
32	.770	.244	30,030	------	----------	9.00	------	------	--------
33	.781	.108	29,930	------	----------	11.60	------	------	--------
Pull-ups at an altitude of 30,000 ft									
34	0.339	1.274	29,900	1.50	4.35×10^{-3}	1.90	0.321	0.950	l
35	.356	1.196	30,000	1.80	4.29	1.43	.344	.700	m, N
36	.400	1.202	30,150	2.50	4.34	1.90	.372	.610	m
37	.420	1.189	30,050	4.40	6.52	1.30	------	------	m
38	.424	1.114	29,750	2.20	3.13	1.70	.400	.831	m
39	.438	1.173	29,850	3.80	.74	1.50	.399	.57	N
40	.461	1.077	27,700	2.50	2.43	1.30	.436	.995	--------
41	.467	1.155	29,850	4.40	4.71	1.25	------	------	m, L, R
42	.481	1.143	30,150	7.10	7.04	1.20	.452	.816	N
43	.512	1.160	30,000	5.90	4.82	1.22	------	------	h
44	.514	1.073	30,000	2.50	2.01	2.20	.467	.829	m
45	.532	1.115	29,850	4.00	2.92	1.40	.500	.830	h
46	.556	1.125	30,050	3.40	2.16	1.90	.509	.800	m
47	.559	1.104	27,500	3.00	1.63	2.50	.504	.790	m
48	.562	1.211	30,100	9.30	5.79	.95	------	------	m, L, R
49	.612	1.082	30,000	3.00	1.41	1.10	.587	.500	h
50	.614	1.147	30,200	6.00	2.88	1.20	------	------	h, L, R
51	.639	1.072	30,400	7.90	3.41	.95	.620	.885	R
52	.666	.956	29,300	------	----------	1.63	.626	.948	h
53	.671	.890	27,000	5.60	----------	1.75	.641	.790	m
54	.685	.830	29,250	------	----------	3.66	.630	.473	h
55	.711	.691	28,850	------	----------	3.60	.648	.659	h
56	.712	.695	29,600	------	----------	1.71	.688	.658	L
57	.726	.620	29,150	------	----------	4.65	.679	.660	m
58	.741	.532	28,700	------	----------	3.03	------	------	h
59	.742	.524	28,550	------	----------	5.07	.689	.567	h
60	.742	.460	28,250	------	----------	4.73	.669	.762	--------
61	.763	.290	28,650	------	----------	5.80	.709	.445	--------
62	.784	.267	29,000	------	----------	5.22	.717	.365	h
63	.786	.201	31,050	------	----------	8.40	710	.345	h
64	.786	------	28,650	------	----------	------	------	------	--------
65	.792	.151	29,050	------	----------	8.05	------	------	--------
Turns at an altitude of 25,000 ft									
66	0.289	1.270	25,400	0.15	0.58×10^{-3}	2.10	------	------	l
67	.315	1.177	24,300	.20	.52	1.70	0.308	0.833	l
68	.315	1.181	24,400	.46	1.25	1.85	------	------	l
69	.320	1.180	25,200	.60	1.52	------	------	------	l
70	.343	1.175	25,000	.60	1.28	1.55	.329	.793	l
71	.360	1.160	24,300	.40	.71	1.72	.368	1.092	l
72	.404	1.128	25,600	.60	.81	1.45	.384	.707	l, R
73	.417	1.105	25,300	.60	.69	------	------	------	m
74	.447	1.101	25,300	1.00	.96	1.80	------	------	m
75	.480	1.075	25,800	1.20	.97	------	------	------	m, R
76	.511	1.060	25,600	1.40	.91	1.40	------	------	m
77	.538	1.044	25,400	1.40	.79	1.35	.512	.730	h
78	.563	1.136	24,600	3.00	1.39	1.05	.544	.640	h
79	.565	1.085	26,100	1.20	.60	.90	.554	.906	h
80	.585	1.136	25,950	4.03	1.83	2.15	------	------	m
Turns at an altitude of 25,000 ft—Concluded									
81	0.678	0.848	27,100	5.40	----------	2.30	0.637	0.816	h
82	.685	.797	27,300	3.05	----------	1.98	.667	.800	l
83	.689	.777	26,500	------	----------	1.98	.702	.600	m
84	.691	.800	24,400	------	----------	1.08	------	------	vl
85	.692	.762	24,950	------	----------	3.32	------	------	l
86	.705	.680	23,700	------	----------	3.50	.704	.710	h
87	.734	.513	26,400	2.20	----------	2.70	.709	.425	h
88	.739	.478	24,980	------	----------	2.65	------	------	l
89	.746	.438	25,400	------	----------	3.55	.734	.380	m
90	.749	.366	27,100	2.10	----------	2.22	.728	.460	l
91	.769	.340	25,200	------	----------	5.70	.745	.428	m
92	.778	.290	25,900	------	----------	------	------	------	l
93	.792	.220	26,800	------	----------	------	------	------	l
Pull-ups at an altitude of 25,000 ft									
94	0.605	1.050	25,500	0.58	0.23×10^{-3}	4.50	0.591	0.930	--------
95	.645	.982	26,100	3.05	1.02	.85	.617	.775	vl
96	.686	.785	26,100	3.05	1.02	1.38	.654	.815	vl
97	.725	.578	26,700	------	----------	5.02	.654	.521	m
Turns at an altitude of 20,000 ft									
98	0.248	1.295	20,100	0.10	0.45×10^{-3}	3.02	------	------	l
99	.256	1.260	19,900	.30	1.17	1.40	0.250	0.570	vl
100	.294	1.221	20,100	.10	.24	1.70	.284	.850	vl
101	.297	1.237	20,500	.62	1.66	1.50	------	------	R
102	.334	1.199	20,380	.805	1.51	1.30	------	------	l, R
103	.337	1.215	20,550	.70	1.31	1.40	------	------	l
104	.345	1.206	20,400	.60	1.03	1.30	------	------	l
105	.348	1.220	20,600	.50	.81	1.28	.351	.881	l
106	.399	1.140	20,300	1.00	1.28	1.08	.395	.655	m
107	.399	1.147	20,650	.805	.90	1.20	------	------	l, R
108	.404	1.149	20,550	2.10	2.24	1.00	------	------	m
109	.440	1.115	20,450	1.40	1.14	1.20	------	------	l
110	.441	1.108	20,900	.805	.67	.95	------	------	--------
111	.453	1.096	20,450	.20	.14	1.00	------	------	l
112	.468	1.090	20,200	1.20	.82	.95	.466	.680	m
113	.506	1.068	19,900	1.40	.73	1.20	------	------	h
114	.508	1.075	20,730	1.73	.93	.90	------	------	l
115	.535	1.073	19,830	2.30	.99	.70	------	------	l
116	.543	1.051	19,650	1.70	.70	.50	------	------	--------
117	.741	.484	18,950	------	----------	1.32	------	------	--------
118	.754	.203	19,900	------	----------	4.70	------	------	l
119	.757	.434	19,400	------	----------	1.6	------	------	l
120	.757	.354	20,600	------	----------	3.60	.730	.500	l
Pull-ups at an altitude of 20,000 ft									
121	0.253	1.388	20,100	1.90	8.30×10^{-3}	2.45	------	------	N
122	.281	1.380	20,250	2.70	8.60	1.70	------	------	--------
123	.317	1.372	20,100	3.90	8.60	1.50	------	------	m
124	.383	1.250	20,150	5.70	7.20	1.40	------	------	h
125	.446	1.100	20,600	2.80	2.17	1.35	0.416	0.718	h
126	.451	1.181	20,100	6.70	5.30	1.12	------	------	h
127	.500	1.081	20,200	3.60	1.98	1.65	.460	.870	--------
128	.526	1.125	20,050	8.10	----------	.90	------	------	m
129	.748	.454	18,950	------	----------	1.82	------	------	vl
130	.759	.375	20,000	------	----------	2.65	------	------	m
Turns at an altitude of 15,000 ft									
131	0.225	1.421	15,350	0.15	0.80×10^{-3}	1.35	------	------	l
132	.247	1.356	15,450	.20	.75	.90	------	------	l
133	.272	1.340	15,350	.60	1.70	1.65	------	------	R
134	.299	1.285	15,800	1.08	2.10	1.67	------	------	R
135	.312	1.251	15,650	.30	.55	1.30	------	------	--------
136	.340	1.232	15,400	1.10	1.55	2.47	------	------	m
137	.365	1.202	15,550	1.40	1.60	3.60	------	------	h
138	.384	1.190	15,850	.80	.80	2.52	------	------	h
139	.409	1.167	15,650	1.70	1.40	3.53	------	------	m
140	.439	1.143	16,100	1.80	1.20	3.00	------	------	R
141	.466	1.102	15,600	2.10	1.20	2.00	------	------	m
Turns at an altitude of 10,000 ft									
142	0.227	1.383	10,250	0.40	0.33×10^{-3}	3.40	------	------	l
143	.249	1.313	10,400	.20	.57	1.45	------	------	l
144	.278	1.320	10,050	.50	1.01	2.75	------	------	m
145	.296	1.345	10,450	1.86	3.17	2.15	------	------	m
146	.317	1.294	11,150	1.00	1.40	2.40	------	------	l, R, L
147	.334	1.237	10,450	0	0	2.65	------	------	h
148	.360	1.247	10,550	1.40	1.33	3.20	------	------	h
149	.378	1.247	11,350	1.80	1.44	2.60	------	------	h
150	.411	1.162	10,250	2.9	1.83	2.15	------	------	m

[a] Letters used in this column have the following significance:

vl very light buffeting
l light buffeting
m moderate buffeting
h heavy buffeting
L left roll-off
R right roll-off
N no roll

TABLE III.—BUFFETING CONDITIONS AND LOADS OF BASIC AIRPLANE—Continued

(b) Left and Right Wing Loads

Run	Left						Right					
	ΔL, lb	M	q, lb/sq ft	C_N	ΔC_N	Δt_{load}, sec	ΔL, lb	M	q, lb/sq ft	C_N	ΔC_N	Δt_{load}, sec
Turns at an altitude of 30,000 ft												
1	564	0.330	49.1	1.280		0.72	606	0.316	45.6	1.265		2.15
2	536	.328	45.9	1.116		1.96	537	.328	45.9	1.116		1.96
3	505	.316	43.9	1.230		4.07	591	.332	48.5	1.209		1.81
4	534	.350	53.0	1.164		.82	613	3.50	53.0	1.164		.83
5	695	.350	52.3	1.135		1.27	585	.351	52.6	1.143		1.24
6												
7	685	.355	55.0	1.124		1.37	612	.349	53.0	1.020		1.68
8	358	.361	56.2	1.102		1.48	318	.361	56.2	1.102		1.24
9	749	.378	63.3	1.115		1.84	728	.378	63.3	1.116		1.85
10	647	.410	70.6	1.108		.30	902	.410	70.6	1.108		.30
11	902	.460	91.0	1.091		.19	793	.460	91.0	1.091		.19
12	567	.475	97.1	1.031		.43	663	.472	95.7	1.025		.59
13	623	.498	111.0	.976		.84	735	.496	111.0	.971		1.32
14	815	.497	106.3	.990		.83	1,032	.497	106.3	.990		.84
15	774	.502	107.5	.985		1.12	726	.503	107.5	.995		.99
16	813	.525	113.1	.955		.44	756	.523	112.2	.933		.56
17	384	.533	119.2	1.003		.83	368	.541	123.1	1.018		.34
18	840	.587	133.9				848	.587	133.9			
19	796	.586	151.2	.950		.50	895	.586	151.2	.945		.55
20	854	.601	163.0	1.000	−0.170	2.00	831	.601	163.0	1.018	−0.152	1.93
21	524	.600	160.5	1.033	−.142	.83	488	.600	160.5	1.044	.131	.66
22	619	.626	158.8				751	.626	158.8			
23	727	.629	182.8	1.054	−.036	2.45	796	.629	182.8	1.054	−.036	2.25
24	1,146	.639	199.7	1.015	−.035	.46	1,319	.640	200.9	1.036	−.009	.25
25	1,165	.634	177.3	1.004	−.066	.78	1,644	.634	177.3	1.004	−.066	.78
26	975	.668	187.2			.19	942	.671	198.9			.62
27	428	.673	199.5			1.60	213	.674	200.1			1.51
28	1,332	.693	216.5			2.02	1,515	.692	216.0			2.61
29	883	.688	241.9	.811	.021	1.38	910	.688	241.9	.811	.021	1.38
30	463	.720	224.0			1.67	550	.717	224.0			1.27
31	317	.759	262.3			1.20	495	.765	265.5			.41
32	519	.761	264.3	.514	.126	2.97	615	.761	264.3	.507	.117	3.93
33	588	.755	290.9	.552	.136	9.81	827	.749	287.5	.603	.149	10.49
Pull-ups at an altitude of 30,000 ft												
34	509	0.337	50.2	1.188		0.32	739	0.331	48.5	0.999		0.89
35	435	.351	54.5	1.155		.42	818	.350	53.9	.970		.69
36	393	.381	63.2	1.032		1.18	877	.382	63.7	1.000		1.08
37	806	.416	75.8	1.375		.28	1,001	.411	73.6	1.104		.69
38	799	.405	73.1	.971		1.23	822	.408	74.1	.991		.95
39	452	.407	73.3	.937		1.04	590	.417	77.0	1.180		.68
40	438	.441	94.9	.955		.98	977	.451	99.3	1.059		.52
41	1,016	.452	90.0	.989		.76	700	.470	97.0	1.081		.17
42	820	.469	95.8	1.194		.45	1,302	.457	91.2	.880		.91
43	1,052	.505	111.5	1.129		.41	822	.505	111.5	1.051		.50
44	1,222	.500	110.2	.931		.86	1,583	.500	110.2	.931		.86
45	832	.514	117.1	.987		.72	1,073	.512	116.4	.970		.80
46	845	.537	126.2	.897		.78	1,164	.535	125.0	.910		.85
47	960	.542	144.8	.920		.84	1,000	.551	149.4	.987		.42
48	1,482	.560	137.0	1.109		.21	1,040	.562	138.2	1.058		.65
49	1,046	.596	156.0	.937		.70	1,091	.600	158.0	.936		.59
50	1,200	.610	162.0	1.063		.19	1,037	.606	159.6	1.025	−0.135	.29
51	1,299	.622	166.5	.892	−0.223	.81	1,452	.622	166.4	.892	−.223	.81
52	2,250	.637	182.7	1.014	−.046	1.18	1,764	.636	182.0	1.018	−.042	1.24
53	1,014	.649	211.2	.980	−.026	1.24	1,541	.651	213.1	.970	−.025	1.12
54	1,322	.640	186.4	.986	−.059	3.00	2,181	.653	194.4	.985	−.010	1.46
55	2,349	.663	203.6	.944	.004	2.96	3,943	.663	203.6	.944	.004	2.96
56	952	.693	214.2	.813	.043	1.45	1,131	.693	214.1	.813	.043	1.45
57	598	.716	239.0	.678	.048	1.57	1,019	.684	217.7	.758	−.057	4.31
58	1,315	.731	252.0	.801	.251	.78	1,236	.731	252.0	.791	.236	.77
59	1,354	.690	225.3	.888	.098	4.31	2,152	.690	225.3	.888	.098	4.31
60	883	.694	230.4	.792	.027	3.63	1,031	.682	222.6	.829	−.001	4.09
61	1,444	.722	252.8	.790	.185	4.86	1,344	.722	252.8	.790	.185	4.86
62	1,153	.753	261.0	.665	.238	3.29	1,514	.742	253.4	.770	.274	3.80
63	1,328	.764	268.9	.647	.282	5.22	2,195	.772	274.0	.644	.324	4.73
64	1,128	.758	273.2	.706	.311		1,738	.748	265.7	.708	.253	
65	751	.769	304.2	.532	.196	6.37	917	.775	304.0	.476	.171	5.89
Turns at an altitude of 25,000 ft												
66	469	0.285	44.0	1.131		1.44	490	0.285	44.1	1.129		1.49
67	422	.361	74.0	1.149		.45	411	.361	74.2	1.135		.57
68	612	.313	55.6	1.125		.99	832	.312	55.1	1.001		1.36
69	455	.310	52.5	1.211		.48	713	.315	54.0	1.195		.31
70	542	.329	59.1	1.188		.75	537	.330	60.0	1.242		.53
71	422	.361	74.0	1.149		.45	411	.361	74.2	1.135		.57
72	965	.388	80.4	1.140		.60	586	.387	80.5	1.136		.63
73	605	.407	90.3	1.078		.72	713	.407	90.3	1.078		.72
74	584	.441	105.3	1.058		.65	562	.441	105.3	1.058		.65
75	628	.470	116.7	1.059		.48	778	.458	111.5	.939		.94
76	706	.492	129.3	.958		.77	1,132	.491	129.0	.955		.81
77	946	.518	145.0	1.029		.75	822	.518	145.0	1.029		.80
78	999	.552	170.0	.968		.57	1,099	.552	170.0	.968		.57
79	536	.559	163.4	1.015		.27	652	.559	163.4	1.006		.32
80	980	.576	175.0	.963		.75	963	.573	173.6	.929		1.01
81	2,136	0.656	215.5	0.967	0	1.36	1,981	0.655	215.0	0.969	−0.006	1.38
82	754	.676	227.0	.830	−.025	.88	842	.676	226.5	.828	−.040	.93
83	482	.699	250.2	.768	.033	1.44	387	.699	291.8	.768	.033	1.23
84												
85	1,204	.673	253.9	.913	.023	2.83	1,334	.678	256.8	.678	.110	2.30
86	1,025	.700	285.2	.748	.023	3.33	926	.704	285.5	.705	−.005	1.30
87	2,524	.717	264.7	.878	.253	1.65	3,016	.715	263.0	.891	.251	1.70
88	681	.722	293.0	.652	.047	2.33	990	.724	292.8	.745	.155	1.89
89	758	.736	291.5	.673	.148	2.84	823	.736	291.8	.673	.148	2.78
90	615	.741	273.7	.614	.122	1.12	555	.739	271.0	.627	.127	1.23
91	389	.759	313.3	.411	.019	1.54	383	.765	315.7	.435	.070	1.18
92	710	.774	313.9	.420	.110	2.91	822	.774	314.0	.402	.092	2.83
93	1,238	.764	297.0	.627	.262	3.43	1,114	.767	300.0	.660	.305	3.19
Pull-ups at an altitude of 25,000 ft												
94												
95												
96												
97	1,219	0.667	224.8	0.870	−0.050	4.55	1,316	0.667	224.8	0.870	−0.050	4.55
Turns at an altitude of 20,000 ft												
98	277	0.232	36.2	1.256		2.29	460	0.237	37.7	1.265		1.99
99	339	.249	42.4	1.245		.74	348	.249	42.4	1.288		.57
100	216	.283	54.3	1.212		.82	246	.283	54.3	1.175		.90
101	454	.288	55.3	1.249		.70	601	.288	55.3	1.249		.70
102	745	.337	76.3	1.138		.59	655	.337	76.3	1.065		.68
103	683	.321	68.9	1.194		.76	607	.320	68.7	1.093		.93
104	451	.338	76.9	1.150		.42	719	.339	77.1	1.268		.38
105	501	.347	79.8	1.242		.29	675	.347	79.8	1.242		.30
106	479	.393	104.0	.980		.76	589	.393	104.0	.961		.77
107	678	.397	104.3	1.111		.30	810	.397	104.3	1.111		.30
108	700	.400	107.1	1.105		.52	907	.400	107.4	1.076		.74
109	842	.430	125.1			.64	924	.435	126.3	1.078		.37
110	627	.437	126.0	1.024		.80	779	.438	126.0	1.045		.68
111	321	.452	137.4			.68	475	.452	137.2	1.030		.60
112	544	.466	146.8	1.047		.36	934	.466	146.8	1.047		.36
113	936	.497	168.6	1.030		.54	900	.497	168.6	1.030		.54
114	841	.508	169.8	.983		.50	1,016	507	169.9	.982		.51
115	298	.534	195.8	.998		.42	450	.534	195.8	.998		.42
116							246	.543	203.2	1.006		.29
117	465	.740	389.8	.505	0.005	.29	347	.744	388.4	.502	0.022	.10
118	279	.737	388.6	.534	.024	4.72	420	.740	389.9	.572	.072	4.42
119	484	.755	406.8	.451	.031	.30	452	.757	408.1	.434	.024	.10
120	259	.745	407.1	.500	.026	1.12						
Pull-ups at an altitude of 20,000 ft												
121	690	0.237	37.9	1.306		0.82	714	0.237	37.9	1.180		0.94
122	612	.271	53.1	1.180		.51	805	.271	53.1	1.228		.41
123	559	.304	62.9	1.160		.60	638	.302	61.5	1.021		.81
124	1,509	.372	92.7	1.190		.54	810	.367	90.3	1.035		.77
125	1,081	.430	122.8	1.029		.70	1,003	436	126.5	1.060		.41
126	1,204	.448	135.5	1.147		.26	778	.435	127.5	1.007		.74
127	409	.476	153.0	1.005		.84	787	.478	154.0	.992		.78
128												
129	523	.740	393.1	.566	0.066	1.02	456	.742	395.5	.563	0.073	.82
130	421	.745	381.9	.542	.067	1.31	464	.748	384.5	.539	.081	1.13
Turns at an altitude of 15,000 ft												
131	297	0.219	39.6	1.309		0.40	438	0.219	39.6	1.309		0.44
132	293	.245	49.3	1.350		.17	478	.245	49.3	1.313		.23
133	375	.272	61.0	1.333		.21	450	.272	61.0	1.303		.25
134	567	.298	72.4	1.070		1.01	570	.301	73.9	1.049		1.10
135	531	.307	78.2	1.197		.82	665	.307	78.2	1.197		.83
136	634	.334	92.5	1.133		1.49	700	.334	92.5	1.133		1.49
137	1,394	.352	102.9	1.107		2.75	857	.353	103.1	1.068		2.54
138	1,004	.380	117.5	1.077		.68	1,023	.380	117.5	1.077		.69
139	964	.406	136.6	1.059		1.86	1,112	.406	136.6	1.059		1.88
140	786	.425	147.0	1.052		2.73	735	.429	148.7	1.095		1.25
141	1,035	.454	170.4	1.039		1.48	923	.454	170.4	1.039		1.48
Turns at an altitude of 10,000 ft												
142	493	0.220	49.0	1.133		2.19	420	0.232	54.4	1.158		1.68
143	726	.242	59.3	1.092		1.17	713	.244	60.3	1.106		1.05
144	722	.271	75.1	1.182		1.06	904	.272	75.7	1.174		.94
145	829	.299	89.4	1.241		.39	1,288	.299	89.6	1.238		.34
146	734	.319	99.3	1.267		.36	905	.319	99.1	1.269		.37
147	973	.340	117.2	1.041		3.27	1,028	.337	114.9	1.126		1.68
148	1,336	.349	123.3	1.033		1.66	1,209	.345	121.0	1.008		2.33
149	893	.375	143.1	1.123		1.53	899	.376	144.0	1.103		1.60
150	867	.414	173.4	1.075		.52	818	.414	173.4	1.086		.44

TABLE III.—BUFFETING CONDITIONS AND LOADS OF BASIC AIRPLANE—Concluded

(c) Left and Right Tail Loads

Run	Left						Right					
	ΔL, lb	M	q, lb/sq ft	C_N	ΔC_N	Δt_{load}, sec	ΔL, lb	M	q, lb/sq ft	C_N	ΔC_N	Δt_{load}, sec
Turns at an altitude of 30,000 ft												
1	402	0.324	47.7	1.180	------	1.38	365	0.338	47.8	1.198	------	1.33
2	120	.330	46.4	1.142	------	1.76	164	.330	46.4	1.142	------	1.70
3	421	.316	43.9	1.141	------	4.20	387	.348	43.9	1.141	------	4.20
4	148	.347	52.2	1.141	------	1.20	182	.347	52.2	1.141	------	1.20
5	------	------	------	------	------	------	------	------	------	------	------	------
6	74	.366	59.5	1.143	------	.26	88	.368	59.6	1.148	------	.15
7	468	.349	53.0	1.020	------	1.69	456	.355	55.0	1.130	------	1.39
8	208	.361	56.2	1.102	------	1.35	247	.361	56.2	1.076	------	1.29
9	515	.374	62.1	1.119	------	2.29	518	.377	63.0	1.121	------	2.01
10	269	.410	70.8	1.108	------	.28	307	.419	69.8	1.105	------	.44
11	509	.456	89.1	1.078	------	.39	462	.460	89.8	1.085	------	.28
12	252	.467	93.7	1.025	------	.86	311	.486	93.4	1.028	------	.90
13	393	.500	111.7	.979	------	.27	376	.499	111.4	.985	------	.73
14	452	.498	106.7	.986	------	.73	470	.500	107.6	.991	------	.52
15	479	.505	108.2	.961	------	.81	426	.505	108.2	.961	------	.82
16	477	.524	112.6	.948	------	.49	595	.530	112.4	.938	------	.54
17	301	.537	121.1	1.005	------	.62	370	.542	119.5	1.003	------	.77
18	501	.586	138.2	------	------	.24	563	.586	138.2	------	------	.30
19	550	.589	152.9	.980	------	.37	587	.595	152.9	.980	------	.40
20	421	.601	162.8	1.020	------	1.92	317	.602	162.9	.989	------	2.0
21	215	.603	162.1	1.045	------	.48	134	.600	160.5	1.044	------	.63
22	467	.627	159.1	------	------	.34	287	.633	160.8	------	------	.17
23	272	.621	179.2	.993	------	2.59	130	.621	179.2	.983	------	2.72
24	567	.640	200.6	1.029	−0.031	.34	588	.645	201.0	1.035	------	.26
25	614	.642	181.7	1.000	−.047	.36	613	.650	178.1	1.004	0.049	.68
26	446	.669	193.4	------	------	.38	298	.666	194.0	------	------	.48
27	302	.672	198.9	------	------	1.66	204	.674	199.3	------	------	1.61
28	658	.693	217.0	------	------	1.98	521	.694	216.8	------	------	1.65
29	248	.695	244.8	.772	.017	.64	248	.695	244.8	.772	.022	.64
30	440	.720	228.3	------	------	1.66	362	.719	224.9	------	------	1.22
31	296	.759	262.4	------	------	1.15	254	.768	263.7	------	------	.82
32	229	.760	263.6	.522	.130	4.01	195	.761	264.3	.500	.115	3.88
33	259	.748	287.1	.604	.149	10.58	248	.750	287.9	.533	.093	10.42
Pull-ups at an altitude of 30,000 ft												
34	415	0.332	48.7	1.015	------	0.83	520	0.335	49.5	1.130	------	0.50
35	430	.351	54.3	1.136	------	.48	449	.349	53.4	.960	------	.94
36	504	.388	65.9	.994	------	.76	520	.383	64.5	.968	------	.94
37	835	.414	75.3	1.340	------	.41	749	.416	75.7	1.375	------	.30
38	387	.415	75.3	1.045	------	.60	621	.413	75.6	.990	------	.72
39	571	.421	78.4	1.250	------	.57	777	.432	82.2	1.289	------	.22
40	513	.444	97.0	1.018	------	.76	510	.444	97.0	1.008	------	.79
41	719	.454	91.0	1.030	------	.70	578	.456	91.8	1.056	------	.57
42	875	.469	96.5	1.194	------	.45	864	.468	95.9	1.180	------	.51
43	730	.499	108.7	1.036	------	.82	687	.505	111.5	1.129	------	.38
44	831	.499	109.5	.942	------	.79	777	.502	111.2	1.006	------	.65
45	781	.515	117.6	.997	------	.66	774	.517	118.3	1.009	------	.58
46	619	.537	126.5	.910	------	.76	766	.543	129.5	.970	------	.56
47	582	.517	131.5	1.040	------	1.80	614	.549	148.5	.955	------	.48
48	805	.560	137.0	1.118	------	.20	734	.556	134.5	1.011	------	.44
49	651	.608	164.0	1.025	------	.18	519	.603	159.8	.980	------	.43
50	613	.597	153.2	1.976	------	.72	637	.596	152.9	.973	------	.76
51	901	.629	170.3	.955	------	.49	667	.630	170.7	.962	------	.57
52	783	.637	183.0	1.013	------	1.18	667	.639	184.1	1.001	------	1.13
53	458	.645	209.5	.938	−0.090	1.38	458	.645	209.5	.937	------	1.39
54	755	.682	212.0	.895	.074	.46	639	.681	211.8	.902	0.072	.58
55	724	.673	209.4	.940	.066	2.57	832	.674	210.2	.930	.060	2.52
56	534	.696	216.4	.876	.134	1.23	621	.697	217.7	.884	.144	1.11
57	472	.714	238.6	.700	.058	2.03	562	.713	258.0	.711	.056	2.39
58	926	.729	250.0	.816	.256	.90	786	.729	250.7	.812	.252	.91
59	724	.695	229.7	.847	.098	3.82	600	.696	231.0	.832	.087	3.71
60	724	.712	244.3	.792	.139	2.72	675	.716	247.0	.752	.127	2.50
61	839	.719	249.4	.755	.140	5.09	801	.719	250.0	.783	.168	5.04
62	778	.737	249.0	.763	.246	4.04	807	.742	253.4	.769	.279	3.82
63	1,040	.765	269.5	.654	.295	5.16	1,000	.768	272.0	.680	.410	4.62
64	940	.755	270.0	.728	.315	------	940	.753	269.0	.732	.302	------
65	655	.785	308.7	.450	.205	5.12	634	.785	308.7	.450	.205	5.12
Turns at an altitude of 25,000 ft												
66	151	0.285	44.1	1.173	------	1.17	132	0.286	44.1	1.256	------	0.75
67	------	------	------	------	------	------	------	------	------	------	------	------
68	278	.312	55.1	1.167	------	.87	294	.312	55.1	1.167	------	.88
69	282	.272	50.3	1.139	------	.76	360	.307	51.6	1.193	------	.64
70	265	.329	59.5	1.231	------	.58	538	.329	59.5	1.220	------	.61
71	181	.360	73.5	1.162	------	.36	138	.359	73.5	1.168	------	.30
72	577	.389	81.2	1.161	------	.48	570	.389	81.0	1.157	------	.53
73	270	.414	92.9	1.095	------	.42	266	.414	92.9	1.092	------	.45
74	503	.438	104.2	1.020	------	.87	467	.440	104.7	1.040	------	.75
75	466	.470	116.7	1.069	------	.38	542	.465	114.2	1.032	------	.65
76	460	.503	133.8	1.037	------	.40	467	.492	129.5	.958	------	.75
77	375	.518	145.0	1.022	------	.80	463	.518	145.0	1.027	------	.82
76	508	.558	174.0	1.014	------	.26	495	.555	172.0	1.000	------	.37
79	453	.560	163.6	1.018	------	.25	408	.560	163.6	1.022	------	.23
80	305	.577	175.4	.961	------	.71	314	.576	175.0	.963	------	.75

Run	Left						Right					
	ΔL, lb	M	q, lb/sq ft	C_N	ΔC_N	Δt_{load}, sec	ΔL, lb	M	q, lb/sq ft	C_N	ΔC_N	Δt_{load}, sec
Turns at an altitude of 25,000 ft—Concluded												
81	939	0.658	216.8	0.960	−0.003	1.27	943	0.647	209.4	0.980	−0.030	1.67
82	515	.674	225.6	.830	−.040	1.18	475	.674	225.6	.830	−.045	1.18
83	397	.698	250.4	.771	.031	1.39	263	.698	250.4	.766	.026	1.46
84	139	.687	266.8	.828	.028	.27	112	.687	266.8	.822	.017	.29
85	346	.674	254.2	.933	.063	2.60	263	.673	253.9	.927	.052	2.71
86	453	.699	284.0	.828	.088	4.90	411	.698	284.2	.828	.088	5.00
87	850	.709	259.7	.908	.238	1.95	831	.712	261.0	.862	.207	2.10
88	393	.727	294.9	.728	.163	1.53	275	.721	292.0	.722	.127	2.11
89	557	.735	291.5	.659	.134	2.95	726	.748	291.5	.673	.208	2.84
91	477	.733	268.7	.643	.103	1.68	548	.733	268.7	.643	.103	1.68
91	160	.764	316.0	.438	.070	1.10	160	.764	316.0	.438	.070	1.10
92	352	.770	312.4	.451	.119	3.28	429	.770	312.4	.430	.095	3.33
93	734	.770	301.7	.658	.326	3.00	848	.769	300.8	.666	.326	3.08
Pull-ups at an altitude of 25,000 ft												
94	------	------	------	------	------	------	------	------	------	------	------	------
95	------	------	------	------	------	------	------	------	------	------	------	------
96	------	------	------	------	------	------	------	------	------	------	------	------
97	609	0.705	254.5	0.743	0.050	2.94	616	0.684	238.6	0.845	0.030	3.86
Turns at an altitude of 20,000 ft												
98	167	0.231	36.2	1.165	------	2.40	187	0.237	38.3	1.182	------	1.90
99	146	.249	42.4	1.261	------	.69	172	.249	42.4	1.265	------	.68
100	201	.283	54.3	1.170	------	.93	236	.283	54.3	1.180	------	.88
101	67	.287	55.0	1.256	------	.75	83	.287	55.0	1.216	------	.76
102	225	.338	76.3	.993	------	.83	180	.338	76.3	1.022	------	.77
103	113	.322	69.0	1.296	------	.65	163	.321	68.9	1.270	------	.81
104	185	.336	76.0	1.098	------	.61	130	.337	76.3	1.158	------	.55
105	214	.346	79.5	1.211	------	.49	281	.345	79.4	1.180	------	.57
106	261	.392	103.0	1.136	------	.46	323	.392	103.0	1.140	------	.44
107	144	.396	103.5	1.099	------	.55	119	.396	103.5	1.099	------	.60
108	236	.400	107.1	.989	------	.93	174	.400	107.1	1.103	------	.53
109	215	.430	125.1	1.064	------	.61	214	.431	125.1	1.061	------	.52
110	110	.438	125.9	1.080	------	.35	169	.438	125.9	1.063	------	.43
111	210	.453	137.1	1.057	------	.37	189	.452	137.0	1.030	------	.49
112	378	.466	146.8	1.058	------	.30	450	.467	146.8	1.081	------	.21
113	562	.497	168.6	1.030	------	.54	552	.496	168.3	1.026	------	.59
114	191	.508	169.8	1.023	------	.27	160	.508	169.8	1.023	------	.29
115	198	.534	195.8	.998	------	.37	114	.534	195.8	.998	------	.38
116	100	.543	203.8	1.029	------	.12	94	.543	203.5	1.026	------	.18
117	104	.740	389.8	.505	0.003	.30	67	.740	389.8	.512	0.012	.34
118	155	.740	389.9	.572	.070	4.39	155	.738	390.3	.545	.040	4.57
119	143	.756	407 7	.450	.035	.2	126	.755	407.2	.451	.036	.3
120	127	.733	387.5	.562	.022	3.0	116	.733	387.5	.562	.017	2.9
Pull-ups at an altitude of 20,000 ft												
121	272	0.237	37.9	1.237	------	0.87	255	0.236	37.5	1.194	------	0.94
122	231	.258	44.8	.879	------	1.30	222	.260	45.3	.844	------	1.23
123	320	.304	62.3	1.119	------	.66	356	.304	62.3	1.084	------	.71
124	321	.368	91.5	1.106	------	.69	377	.370	92.7	1.155	------	.58
125	822	.433	124.5	1.047	------	.52	641	.432	124.2	1.040	------	.58
126	441	.437	128.3	1.038	------	.69	434	.437	128.3	1.038	------	.69
127	519	.483	157.0	1.009	------	.60	495	.478	154.0	.992	------	.78
128	------	------	------	------	------	------	------	------	------	------	------	------
129	170	.736	389.7	.574	0.049	.73	170	.738	390.1	.559	0.057	.57
130	152	.750	386.7	.522	.072	.68	181	.748	385.5	.539	.084	1.13
Turns at an altitude of 15,000 ft												
131	145	0.216	38.5	1.193	------	0.61	162	0.220	40.1	1.304	------	0.24
132	145	.242	48.4	1.238	------	.33	124	.242	48.4	1.238	------	.34
133	199	.269	60.0	1.231	------	.74	137	.269	60.0	1.231	------	.74
134	162	.293	70.1	1.158	------	.78	148	.294	70.5	1.124	------	.81
135	55	.309	78.6	1.170	------	.91	51	.309	78.7	1.169	------	.89
136	263	.333	91.6	1.124	------	1.17	207	.335	93.0	1.128	------	1.63
137	508	.351	102.4	1.112	------	2.83	343	.354	103.8	1.079	------	2.23
138	216	.380	117.3	1.107	------	.52	292	.382	119.3	1.045	------	1.89
139	306	.401	133.2	1.086	------	1.75	382	.406	136.8	1.030	------	2.02
140	298	.437	153.3	1.073	------	.34	269	.437	153.3	1.073	------	.33
141	248	.454	170.1	1.041	------	1.28	214	.456	171.2	1.045	------	1.16
Turns at an altitude of 10,000 ft												
142	302	0.234	55.3	1.205	------	0.60	318	0.233	54.8	1.284	------	1.13
143	321	.247	61.2	1.179	------	.77	273	.247	61.6	1.172	------	.74
144	318	.275	77.6	1.145	------	1.62	436	.276	78.1	.995	------	1.81
145	281	.297	89.1	1.121	------	1.26	269	.297	89.1	1.120	------	1.69
146	297	.318	98.6	1.126	------	.79	305	.317	98.1	1.056	------	.50
147	407	.340	117.1	1.058	------	2.09	361	.340	117.2	1.041	------	2.10
148	458	.352	124.6	1.097	------	1.23	394	.352	124.7	1.096	------	1.24
149	500	.377	144.8	1.072	------	1.89	363	.376	144.0	1.090	------	1.82
150	330	.414	173.4	1.096	------	.43	293	.414	173.4	1.096	------	.43

TABLE IV.—BUFFETING CONDITIONS AND LOADS OF MODIFIED AIRPLANE

(a) Operating Conditions

Run	M_B	C_{N_B}	h_p, ft	$\dot{n}$	$\frac{\dot{\alpha}\bar{c}}{V}$	Δt, sec	M_E	C_{N_E}	Pilot's note (a)
Pull-ups at an altitude of 30,000 ft									
1	0.275	1.194	29,900	0.10	0.53×10^{-3}	4.25	0.236	1.177	l,L, R
2	.287	1.201	29,900	.50	2.35	1.90	.273	0	vl
3	.287	1.197	29,900	.20	.94	8.12	.249	.984	vl
4	.298	1.250	29,900	.60	2.51	1.85	.287	.701	-------
5	.327	1.226	29,800	.50	1.58	3.80	.298	.601	l
6	.354	1.147	30,300	.60	1.52	2.90	.327	.765	m
7	.377	1.154	29,900	.80	1.65	3.50	.324	.791	l
8	.421	1.083	30,300	1.10	1.65	3.53	.357	.728	m
9	.452	1.093	30,400	1.10	1.36	3.30	.387	.863	m
10	.469	1.094	30,900	1.10	1.24	4.13	.368	.815	m
11	.474	1.103	29,800	2.40	2.48	3.00	.405	.524	h, R, L
12	.476	1.115	30,200	2.20	2.28	2.60	.403	.840	-------
13	.479	1.128	30,100	7.70	7.80	2.40	.416	.951	-------
14	.480	1.100	30,400	1.60	1.64	2.60	.414	1.023	m, R, L
15	.483	1.088	30,200	1.50	1.49	2.70	.381	.902	h, R, L
16	.490	1.092	31,400	2.20	2.22	4.00	.399	.848	m
17	.511	1.107	29,600	2.80	1.17	2.20	.469	.783	h
18	.513	1.085	29,200	1.70	.69	3.20	.443	.644	h
19	.516	1.080	30,300	.90	.75	2.00	.465	1.050	m
20	.516	1.072	30,300	1.00	.90	2.70	.466	.758	h
21	.537	1.078	30,700	1.40	1.04	2.40	.493	.858	h, R, L
22	.541	1.072	30,900	1.00	.73	4.2	.436	.941	m, R, L
23	.548	1.087	31,900	2.10	1.55	2.00	.505	.648	m, R, L
24	.716	.629	28,800	-----	----------	1.50	.691	.705	l
25	.743	.512	28,500	-----	----------	3.10	.708	.667	-------
26	.758	.400	29,000	-----	----------	-----	.696	.739	-------
27	.763	.332	28,200	-----	----------	5.70	.724	.580	m
28	.768	.385	29,000	-----	----------	-----	.708	.671	h
29	.769	.423	29,300	-----	----------	5.40	.697	.720	l
30	.771	.340	28,600	-----	----------	7.00	.705	.690	m
31	.771	.429	29,700	-----	----------	5.50	.695	.677	l
32	.773	.279	28,900	-----	----------	-----	.696	.740	l
33	.777	.334	28,300	-----	----------	6.50	.704	.720	l, R
34	.796	.273	28,700	-----	----------	-----	.716	.638	l
Turn at an altitude of 30,000 ft									
35	0.350	1.170	28,000	0.10	0.23×10^{-3}	1.60	0.349	0.977	R
Pull-ups at an altitude of 10,000 ft									
36	0.168	1.241	10,100	0	0	4.00	0.174	0.699	vl
37	.205	1.308	10,200	.40	2.06×10^{-3}	3.40	1.78	.904	l
38	.207	1.482	9,950	1.50	7.48	2.40	1.84	.620	l
39	.261	1.284	10,100	.70	1.75	1.60	.232	.862	m
40	.267	1.435	9,950	2.00	4.63	1.70	.241	.821	h
41	.267	1.593	10,150	4.00	9.33	1.55	.247	.468	h
42	.332	1.229	10,700	.70	.87	1.35	.299	.781	h
43	.337	1.271	10,400	1.60	1.88	2.22	.280	.700	-------
44	.342	1.338	10,100	7.60	8.44	1.15	.329	.298	h

[a] Letters used in this column have the following significance:

vl	very light buffeting	L	left roll-off
l	light buffeting	R	right roll-off
m	moderate buffeting	N	no roll
h	heavy buffeting		

(b) Left and Right Wing Loads

Run	Left						Right					
	ΔL, lb	M	q, lb/sq ft	C_N	ΔC_N	Δt_{load}, sec	ΔL, lb	M	q, lb/sq ft	C_N	ΔC_N	Δt_{load}, sec
Pull-ups at an altitude of 30,000 ft												
1	445	0.261	30	1.208	------	1.98	363	0.262	30	1.198	------	1.82
2	405	.271	32	1.050	------	1.25	420	.278	34	1.341	------	.32
3	300	.277	33	1.007	------	1.92	500	.282	35	1.190	------	.60
4	445	.287	36	.857	------	1.54	670	.294	38	1.248	------	.38
5	445	.323	46	1.175	------	1.92	370	.318	44	1.090	------	1.20
6	386	.328	46	.890	------	2.45	344	.349	53	1.140	------	.60
7	500	.351	54	1.146	------	1.85	575	.357	56	1.073	------	1.42
8	560	.384	64	.861	------	2.09	540	.394	67	1.056	------	1.54
9	613	.402	68	.920	------	2.80	421	.432	80	1.112	------	.80
10	695	.440	81	.894	------	1.40	705	.441	81	1.022	------	1.34
11	605	.425	79	1.025	------	1.70	775	.417	76	.973	------	2.02
12	640	.453	89	1.067	------	.76	785	.458	90	1.068	------	.59
13	810	.458	91	.983	------	.75	745	.463	93	1.005	------	.60
14	735	.468	94	1.048	------	.56	610	.448	86	1.065	------	1.20
15	730	.467	94	1.093	------	.54	700	.431	79	1.102	------	1.65
16	600	.454	84	1.001	------	1.42	640	.434	76	.988	------	2.13
17	965	.487	106	1.020	------	1.18	820	.481	104	1.106	------	1.45
18	800	.450	92	1.109	------	2.59	725	.449	91	1.061	------	2.71
19	710	.497	108	.967	------	.70	845	.497	108	.966	------	.70
20	650	.493	105	.957	------	1.28	560	.492	104	.949	------	1.34
21	607	.530	110	1.010	------	1.50	543	.530	112	1.001	------	1.30
22	825	.501	105	.966	------	1.76	600	.502	105	.960	------	1.75
23	715	.516	106	.971	------	1.39	595	.520	108	.977	------	1.24
24	272	.714	236	.651	0	.20	140	.714	236	.662	0.011	.20
25	355	.718	243	.657	.030	2.48	245	.730	251	.584	.029	1.64
26	325	.752	267	.513	.080	2.44	455	.756	267	.487	.075	1.14
27	214	.724	260	.579	−.012	5.70	265	.740	272	.586	.086	4.70
28	220	.721	256	.607	−.002	6.57	295	.752	279	.421	−.015	3.32
29	440	.721	237	.660	.051	4.01	430	.759	263	.540	.145	1.08
30	382	.763	280	.451	.076	3.10	142	.763	280	452	.080	3.10
31	805	.747	252	.638	.175	2.32	620	.746	251	.635	.166	2.39
32	795	.770	283	.478	.148	2.20	650	.754	275	.578	.157	4.54
33	228	.747	269	.588	.125	3.60	227	.759	278	.513	.118	2.60
34	600	.753	278	.583	.156	5.72	510	.767	287	.520	.169	4.61
Turn at an altitude of 30,000 ft												
35	480	0.350	59	1.156	------	0.40	391	0.350	59	1.145	------	0.40
Pull-ups at an altitude of 10,000 ft												
36	315	0.165	27	1.273	------	2.22	435	0.165	27	1.180	------	2.76
37	510	.196	38	1.254	------	1.01	585	.187	36	1.194	------	1.88
38	785	.200	41	1.411	------	.62	510	.199	40	1.174	------	.69
39	655	.246	61	1.150	------	.80	810	.247	61	1.150	------	.79
40	710	.253	65	1.082	------	.91	830	.261	69	1.175	------	.46
41	850	.257	67	1.130	------	.69	805	.257	67	1.130	------	.72
42	450	.319	100	1.225	------	.50	1,450	.313	96	1.182	------	.76
43	905	.327	90	1.028	------	1.39	1,085	.316	99	1.120	------	.83
44	1,380	.336	114	1.150	------	.39	1,210	.337	114	1.160	------	.38

TABLE IV.—BUFFETING CONDITIONS AND LOADS OF MODIFIED AIRPLANE—Concluded

(c) Left and Right Tail Loads

Run	Left						Right					
	ΔL, lb	M	q, lb/sq ft	C_N	ΔC_N	Δt_{load}, sec	ΔL, lb	M	q, lb/sq ft	C_N	ΔC_N	Δt_{load}, sec
Pull-ups at an altitude of 30,000 ft												
1	266	0.261	30	1.209	------	1.97	285	0.261	30	1.214	------	2.02
2	238	.276	33	1.390	------	.45	375	.275	33	1.402	------	.51
3	310	.278	34	1.012	------	1.76	355	.277	33	1.008	------	1.81
4	350	.287	36	.886	------	1.42	450	.287	36	1.190	------	.94
5	365	.309	42	1.075	------	2.30	450	.318	44	1.090	------	1.20
6	308	.335	48	1.037	------	1.85	546	.335	48	.988	------	1.85
7	400	.342	52	1.085	------	2.37	415	.364	58	1.106	------	.88
8	415	.397	68	1.050	------	1.36	485	.396	68	1.051	------	1.41
9	420	.411	74	1.054	------	2.20	405	.410	71	1.036	------	2.30
10	495	.405	68	1.035	------	2.81	515	.421	74	1.000	------	2.16
11	682	.443	86	1.089	------	1.06	770	.426	79	1.030	------	1.66
12	572	.462	92	1.080	------	.41	605	.419	75	1.040	------	1.94
13	760	.463	93	1.012	------	.58	705	.473	97	1.085	------	.23
14	513	.470	94	1.047	------	.50	539	.462	80	1.096	------	1.76
15	643	.422	76	1.107	------	1.98	705	.418	74	1.109	------	2.13
16	572	.440	79	.980	------	1.92	704	.440	79	.980	------	1.92
17	591	.484	105	1.011	------	1.33	770	.483	105	1.010	------	1.37
18	591	.505	116	1.100	------	.43	660	.470	101	1.010	------	1.61
19	353	.471	96	1.028	------	1.50	361	.471	96	1.028	------	1.50
20	495	.476	96	.930	------	2.25	690	.481	98	.935	------	1.98
21	366	.535	112	1.000	------	1.10	212	.524	116	1.018	------	.70
22	540	.489	106	.960	------	1.71	470	.511	110	.973	------	1.38
23	566	.518	107	.974	------	1.30	517	.520	108	.975	------	1.26
24	206	.714	236	.662	0.011	.20	109	.714	236	.661	0.010	.20
25	260	.736	256	.585	.061	1.01	165	.717	241	.663	0	2.59
26	365	.713	240	.675	.018	6.03	300	.712	239	.677	.014	6.08
27	192	.740	272	.589	.089	4.7	275	.740	272	.589	.089	4.70
28	280	.768	284	.380	0	.47	220	.761	284	.410	.027	2.02
29	435	.756	262	.560	.150	1.28	409	.741	251	.610	.115	2.58
30	165	.763	280	.451	.079	3.10	177	.763	280	.451	.079	3.10
31	487	.748	253	.640	.183	2.26	526	.746	252	.636	.167	2.37
32	345	.754	275	.578	.147	4.56	475	.770	283	.475	.145	2.13
33	415	.750	271	.580	.135	3.40	473	.750	271	.581	.136	3.40
34	409	.772	290	.478	.162	4.12	374	.763	285	.538	.168	4.87
Turn at an altitude of 30,000 ft												
35	173	0.350	59	1.085	------	0.90	269	0.350	59	1.083	------	0.90
Pull-ups at an altitude of 10,000 ft												
36	295	0.165	27	1.290	------	2.04	310	0.165	27	1.180	------	2.77
37	435	.190	36	1.218	------	1.65	517	.194	37	.898	------	1.20
38	505	.200	41	1.410	------	.62	660	.199	40	1.380	------	.69
39	540	.247	61	1.160	------	.74	440	.253	65	1.210	------	.43
40	520	.262	67	1.138	------	.61	640	.259	68	1.147	------	.56
41	595	.263	70	1.380	------	.30	715	.262	69	1.320	------	.39
42	495	.309	86	1.100	------	.94	430	.311	95	1.160	------	.82
43	700	.324	104	1.198	------	.52	595	.320	101	1.160	------	.69
44	915	.334	113	.910	------	.64	715	.336	113	1.080	------	.45

The flight conditions for the onset and end of buffeting given in tables III (a) and IV (a) are summarized in plots of airplane normal-force coefficient against Mach number in figures 4 and 5, respectively. In figure 4 (a) a buffet boundary for the onset of buffeting is also shown and two labels "Stall regime" and "Shock regime" are included. These labels denote speed regimes in which the flight characteristics of the airplane differ and, thus, speed regimes in which the buffet boundary was obtained in different ways. For Mach numbers below about 0.65, buffeting was usually encountered in an accelerated stall maneuver; a maximum value of airplane normal-force coefficient was reached; and controlled flight at still higher load factors was not then possible. In this stall regime the value of C_{N_B} for the onset of buffeting varied with Mach number and also was generally higher in pull-ups than in turns. The increase can be associated with the abruptness of the stall entry, as measured by the largest value of $\dot{\alpha}\bar{c}/V$ reached prior to the onset of buffeting. The

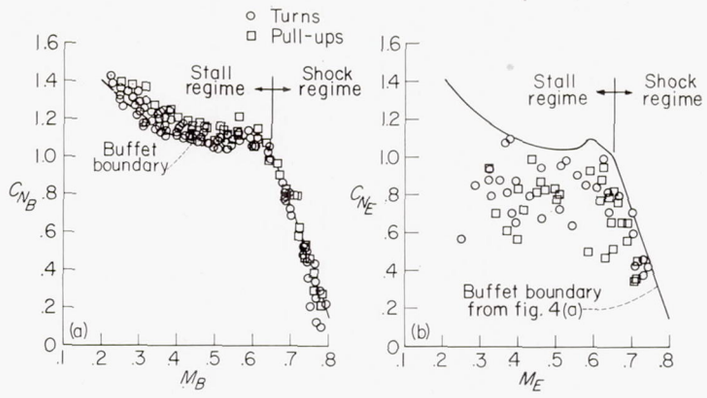

(a) Onset of buffeting. (b) End of buffeting.

FIGURE 4.—Onset and end of buffeting for various maneuvers of basic airplane.

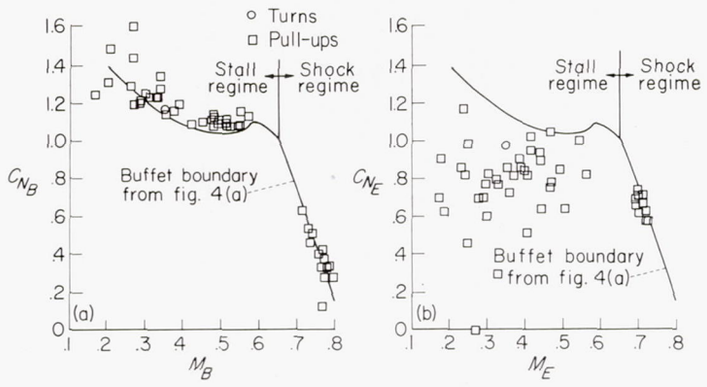

(a) Onset of buffeting. (b) End of buffeting.

FIGURE 5.—Onset and end of buffeting for various maneuvers of modified airplane.

buffet boundary shown for the stall regime in figure 4 (a) was obtained from faired cross plots of C_{N_B}, M, and $\dot{\alpha}\bar{c}/V$, greatest weight being given to the data for 30,000 feet, and corresponds at each Mach number to the value of C_{N_B} for $\dot{\alpha}\bar{c}/V=0$. The difference between this boundary and the actual C_{N_B} at the onset of buffeting is plotted as a function of $\dot{\alpha}\bar{c}/V$ in figure 6 for the data from altitudes of 30,000, 20,000, and 10,000 feet. The increment in normal-force coefficient is analogous to the increment in the dynamic value of the maximum lift coefficient as compared with the static value, but, because of the approximate nature of the relation between accelerometer reading and rate of change of angle of attack, a more detailed study which might include the effects of Reynolds number has not been attempted. For this reason also, no attempt has been made to specify a variation of buffet boundary with altitude, although the possibility of such a variation is suggested by a comparison of the plots for 30,000 feet and 10,000 feet in figure 6.

For Mach numbers above about 0.65, buffeting was encountered during diving turns or in pull-outs from dives. The onset of buffeting occurred at values of C_N well below maximum lift, but controlled flight at normal-force coefficients well above the value for the onset of buffeting was feasible. The buffet boundary shown in figure 4 (a) above $M=0.64$ was obtained by fairing through the observed values of C_{N_B}, greatest weight being given to the data for 30,000 feet.

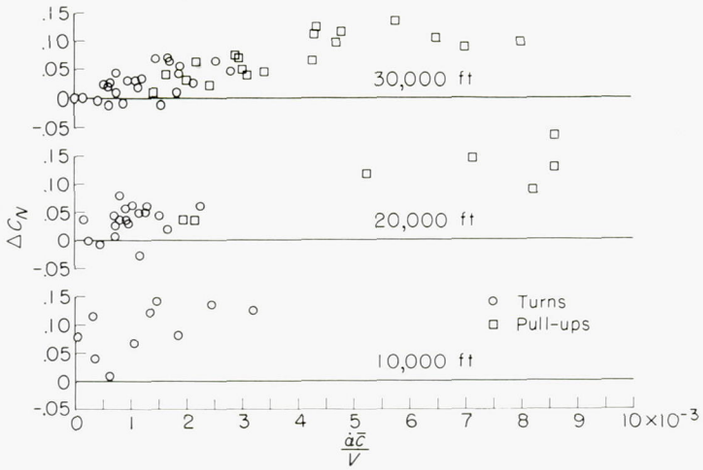

FIGURE 6.—Effect of abruptness of stall entry on C_N at onset of buffeting.

The buffet boundary of figure 4 (a), based on data for the onset of buffeting, appears to define a transition from steady to unsteady phenomena. This boundary, which has been placed in figure 4 (b) for comparison, does not appear to define the transition from unsteady back to steady conditions. The data for the end of buffeting represent, however, the flight conditions on final subsidence of oscillations in the structure. In the shock regime, when buffeting persisted to values of C_N below the buffet boundary and the return to level flight from the maximum load factor was rapid, the persistent fluctuations appeared to differ in character from the rest of the record and to resemble the subsidence of a damped oscillation from which the excitation has been removed. When the approach to the boundary was at a slow rate (generally accomplished by a loss of speed at nearly constant load factor), the end of buffeting occurred as the boundary was crossed. The buffet boundary above $M=0.65$ as defined by the onset of buffeting may, therefore, represent a distinct boundary below which a buffeting excitation is not present.

In the stall regime, values of C_{N_E} in almost all instances are below the buffet boundary. Although the persistence of structural oscillations may be a factor in this case also, the character of the fluctuations indicates that buffeting, once encountered, is maintained to values of C_N reached in the stall recovery which are well below the buffet boundary.

The buffet boundary for the basic airplane, figure 4 (a), has been plotted in figure 5 (a) for comparison with the data for the modified airplane. The boundary for the basic airplane appears to represent the modified airplane reasonably well. The two points for C_{N_B} at the lowest Mach numbers are for maneuvers at 10,000 feet and may represent a Reynolds number effect, but enough data to establish a consistent trend are not available.

WING AND TAIL BUFFETING LOADS

The wing buffet loads associated with the runs of table III (a) and IV (a) are given in tables III (b) and IV (b); the tail buffet loads are given in tables III (c) and IV (c). There is also listed a quantity ΔC_N, the penetration beyond the buffet boundary in terms of mean airplane normal-force coefficient, used in the analysis of some of these data.

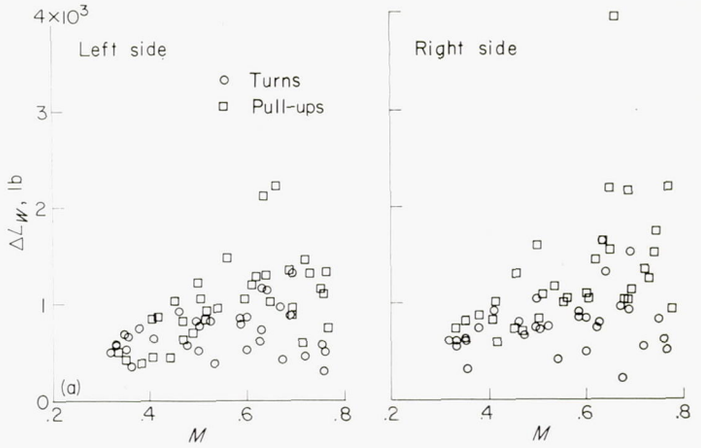

(a) Altitude, 30,000 feet.

FIGURE 7.—Wing buffeting loads of basic airplane.

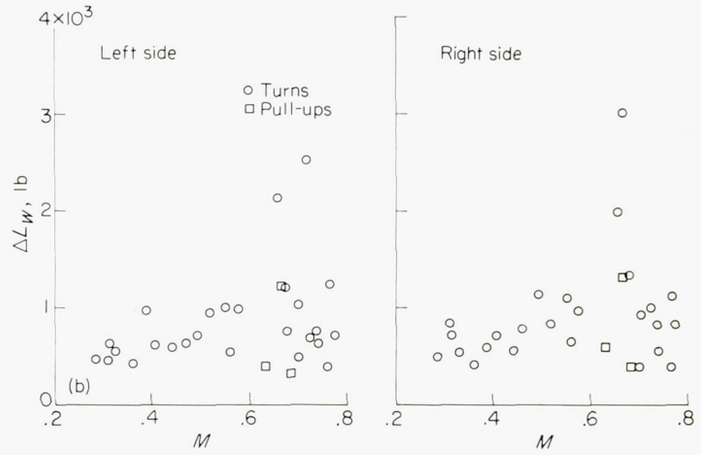

(b) Altitude, 25,000 feet.

FIGURE 7.—Continued.

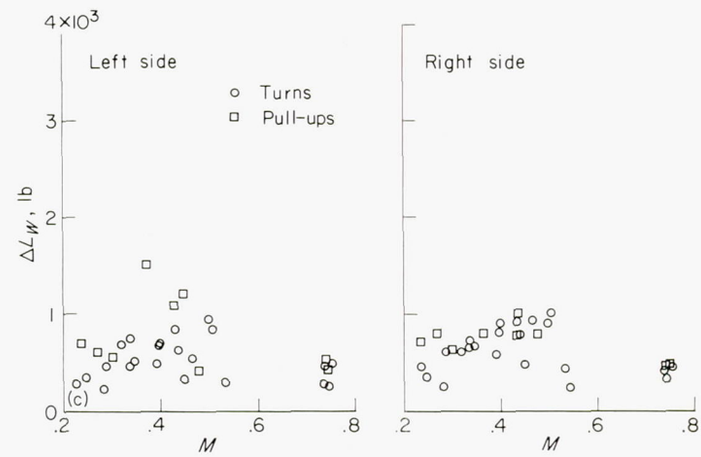

(c) Altitude, 20,000 feet.

FIGURE 7.—Continued.

The wing and tail buffet-load values for the basic airplane given in tables III (b) and III (c) are shown in summary form in figures 7 and 8; the data for the modified airplane are shown in figures 9 and 10. In these figures the variation of the loads on the left and right surfaces with Mach number is shown for each of the nominal test altitudes. Turns are distinguished from pull-ups.

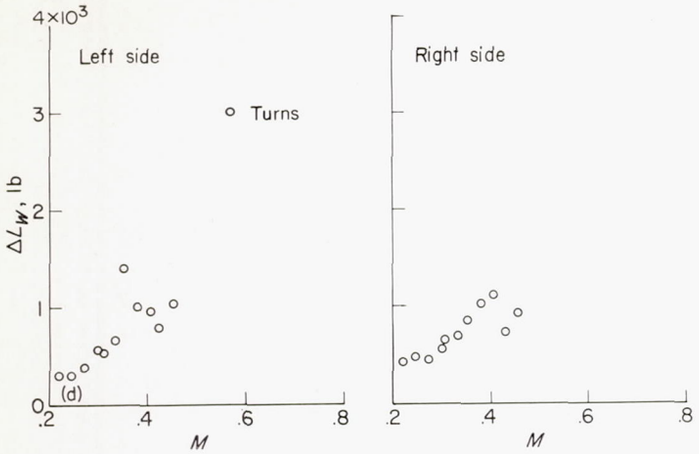

(d) Altitude, 15,000 feet.

FIGURE 7.—Continued.

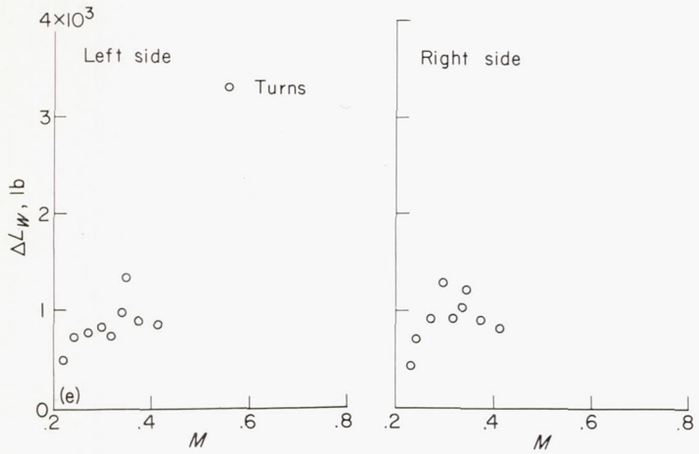

(e) Altitude, 10,000 feet.

FIGURE 7.—Concluded.

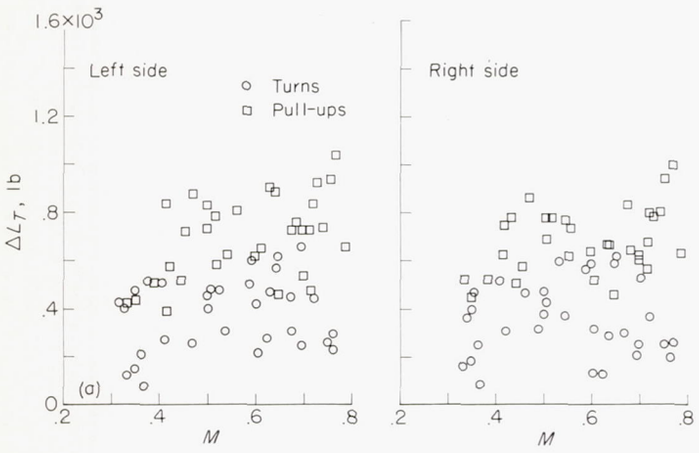

(a) Altitude, 30,000 feet.

FIGURE 8.—Tail buffeting loads of basic airplane.

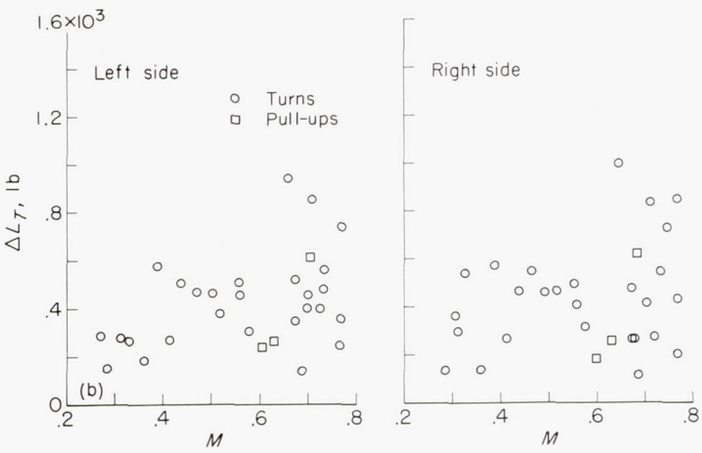

(b) Altitude, 25,000 feet.

FIGURE 8.—Continued.

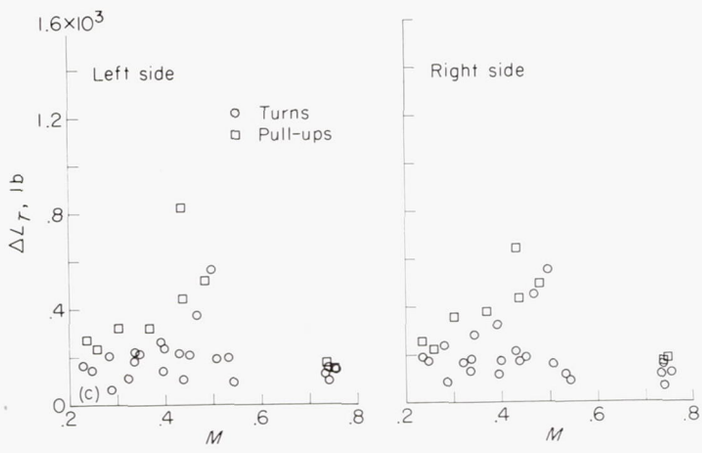

(c) Altitude, 20,000 feet.

FIGURE 8.—Continued.

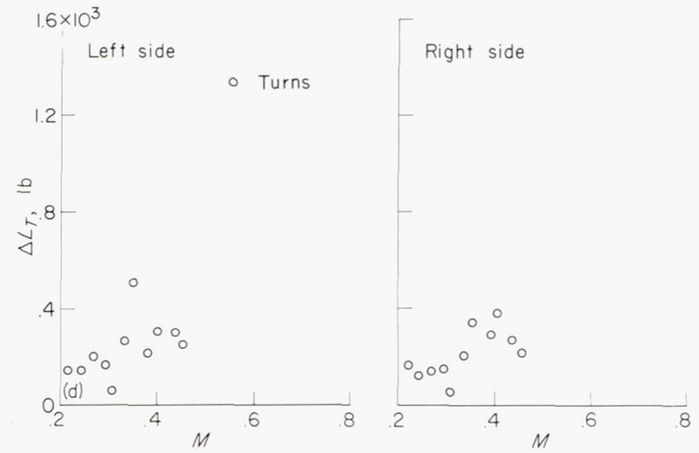

(d) Altitude, 15,000 feet.

FIGURE 8.—Continued.

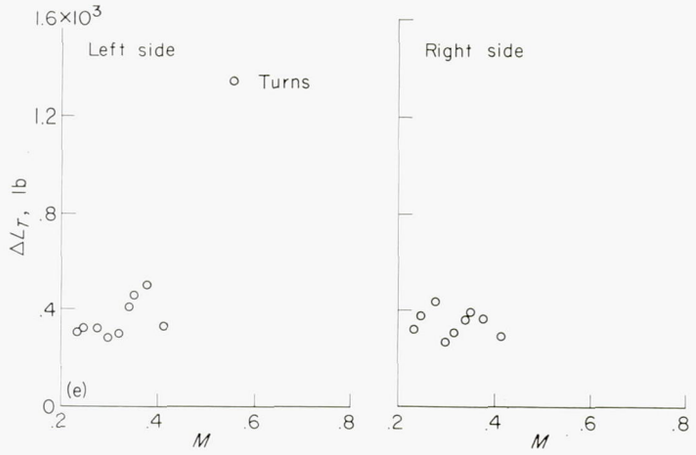

(e) Altitude, 10,000 feet.

Figure 8.—Concluded.

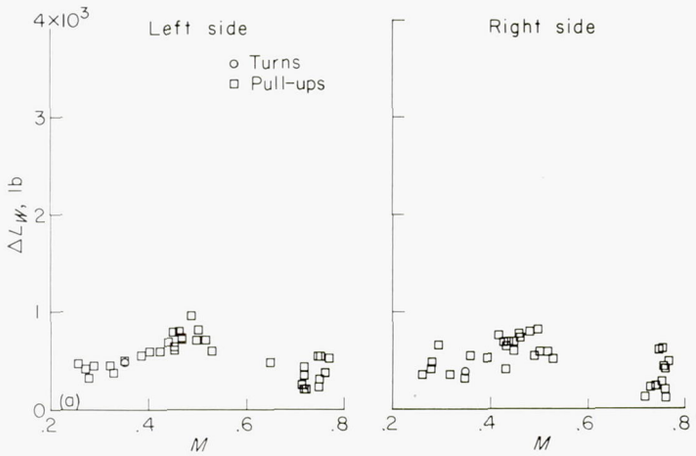

(a) Altitude, 30,000 feet.

FIGURE 9.—Wing buffeting loads of modified airplane.

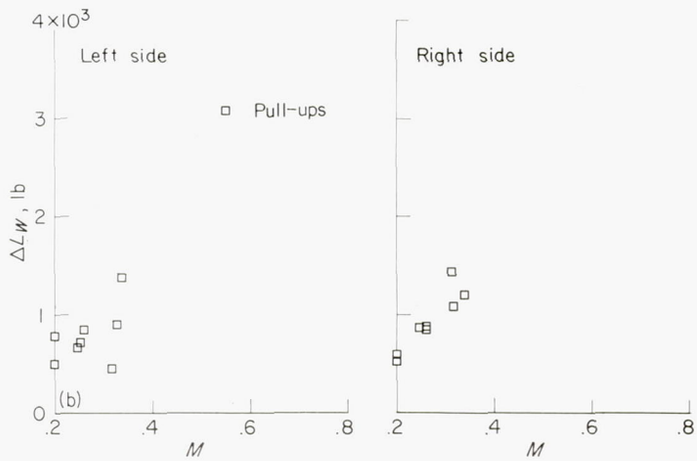

(b) Altitude, 10,000 feet.

FIGURE 9.—Concluded.

In the absence of any accepted theory relating the magnitude of the loads in buffeting to the flight conditions and the characteristics of the structure, the analysis of the load data of tables III and IV has necessarily been of a somewhat qualitative nature, involving both general regression studies and the fitting of regression equations to the data by means of least-squares methods. The results of this study are incorporated in the following section.

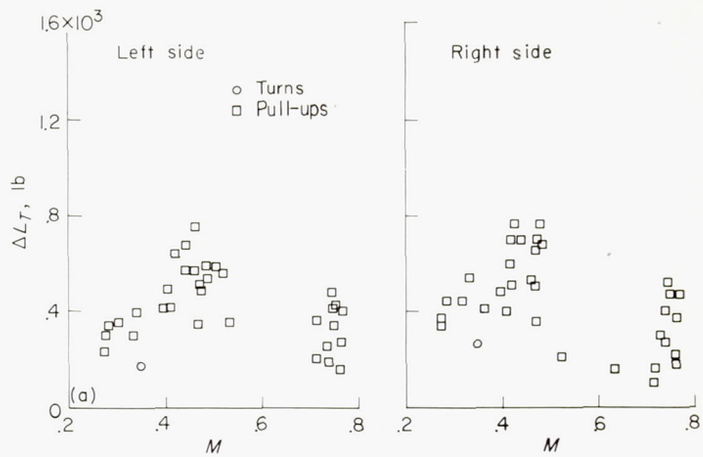

(a) Altitude, 30,000 feet.

FIGURE 10.—Tail buffeting loads of modified airplane.

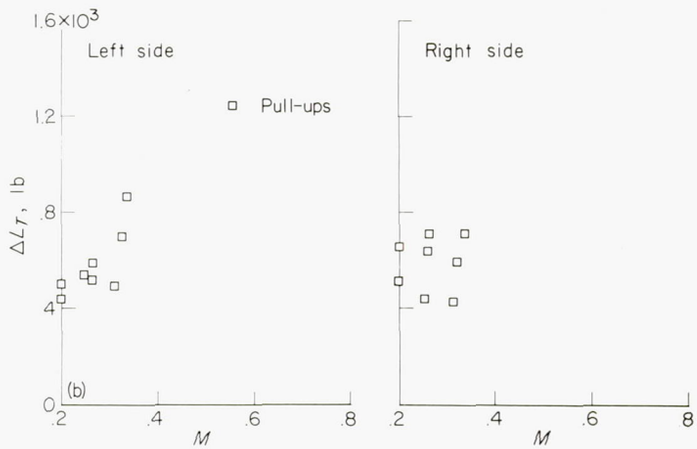

(b) Altitude, 10,000 feet.

FIGURE 10.—Concluded.

ANALYSIS AND DISCUSSION OF BUFFETING-LOAD DATA

When the buffeting-load data of tables III and IV are plotted against Mach number for different altitudes, the large amount of scatter in, for example, figures 7 and 8 makes it difficult to assess the effects of both speed and altitude and suggests that other factors may be significant. As shown by the difference between the data for turns and pull-ups in figure 7 (a), one such factor is the abruptness with which the stall is entered. A number of studies have been undertaken in attempts to identify other significant parameters. In these studies use has been made of the usual methods of regression analysis, including correlation studies, graphical studies, and the fitting of regression equations by least-squares methods. The form of these equations was inferred from the graphical studies or in some instances could be based on analytical results. In these studies the loads measured in stalls were found to follow a somewhat different pattern from those measured in the shock regime.

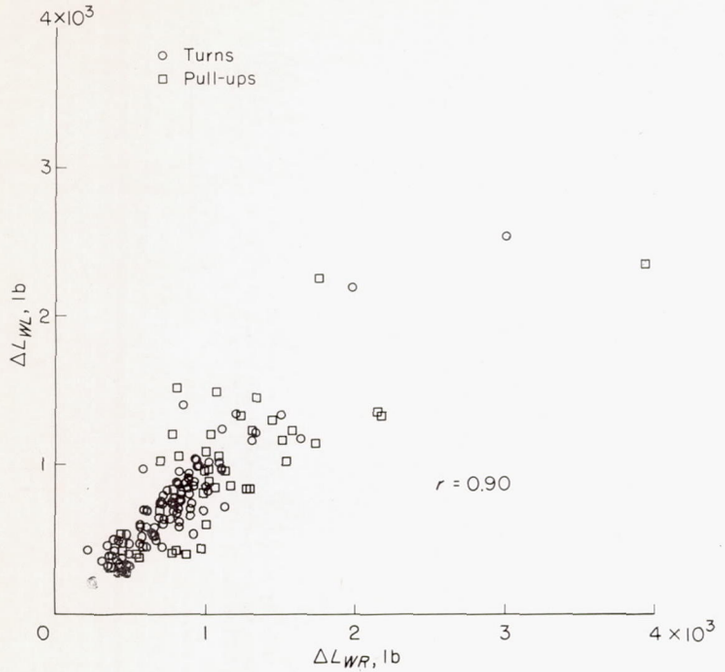

FIGURE 11.—Correlation between left and right wing buffeting loads for basic airplane.

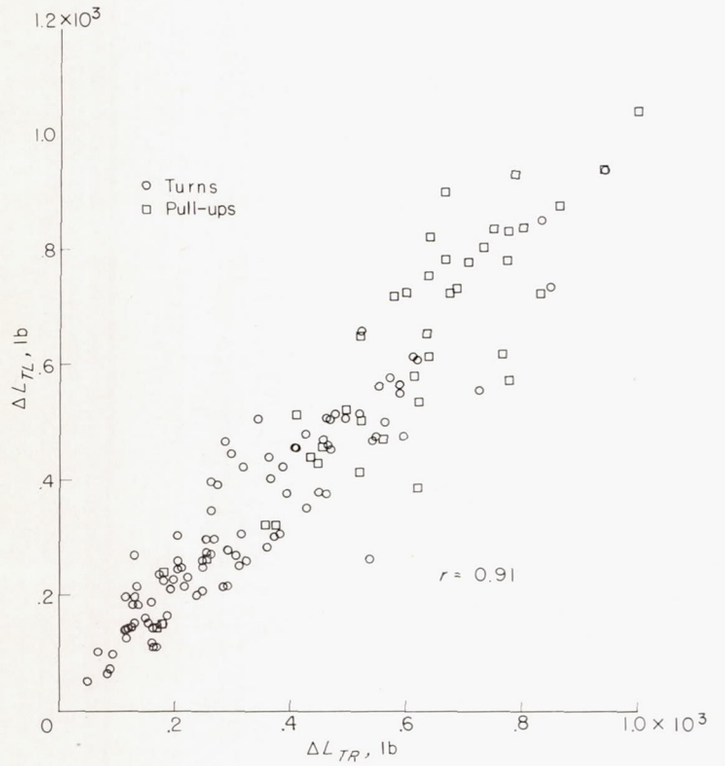

FIGURE 12.—Correlation between left and right tail buffeting loads for basic airplane.

As a preliminary to analysis of the load data, a considerable simplification was effected on the basis of plots of left wing load against right wing load and left tail load against right tail load shown in figures 11 and 12, respectively. The coefficient of correlation shown in these plots, of the order of $r=0.9$, can be regarded as a measure of common causes and suggests that the factors which produce loads of a given size are, in general, common to the left and right wing panels or left and right tail surfaces. On this basis, the mean value ΔL_W of the two wing-panel loads measured in a run was taken as representative of the wing loads encountered during that run; that is, the mean wing load

$$\Delta L_W = 0.5(\Delta L_{WL} + \Delta L_{WR})$$

and a similar mean tail load

$$\Delta L_T = 0.5(\Delta L_{TL} + \Delta L_{TR})$$

were used to represent the loads in each run.

A scatter diagram of ΔL_W against ΔL_T is shown in figure 13. The value of the coefficient of correlation, 0.7, suggests a larger degree of independence between wing and tail loads than is the case for the left and right wing or tail surface. On this account, analysis of the wing and tail loads was carried out independently.

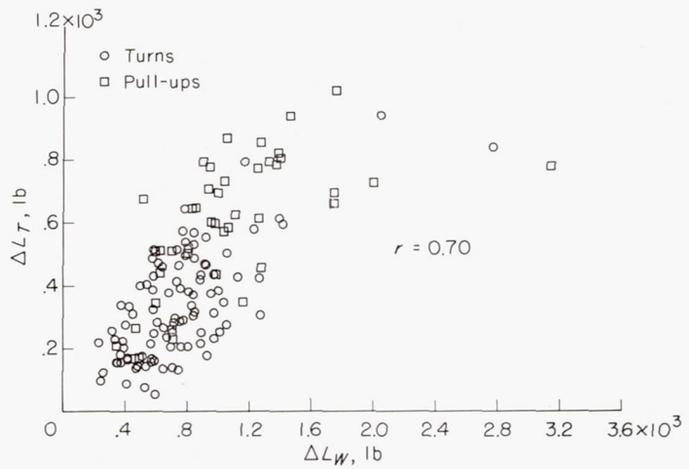

FIGURE 13.—Correlation between wing and tail buffeting loads for basic airplane.

REGRESSION ANALYSIS

When dealing with quantities of data, the interrelation of more than two parameters cannot ordinarily be shown in a simple plot, but the effect of a given independent variable can be investigated if the data are grouped by classes of this variable and the average values of the dependent variable (in the present case the load ΔL) are computed for each class. Provided that each class constitutes a similar sample, the effect of other independent variables on the load may thus be suppressed, or averaged out, and the variation with the independent variable of interest established. The grouping and averaging may then be repeated for other variables. Such an analysis is, of course, somewhat qualitative, and it may be difficult to show the effect of a secondary variable in the presence of a large primary effect.

In the study of loads measured on the basic airplane, the variables investigated for runs in which the stall was reached include dynamic pressure q and the length of time spent in buffeting Δt. Also investigated was the effect of the abruptness of the stall entry. For this investigation the value of $\dot{\alpha}\bar{c}/V$ was used as a measure of the abruptness of the entry in both turns and pull-ups. For buffeting encountered in

the shock regime, the variables investigated include the dynamic pressure and the increment in normal-force coefficient beyond the buffet boundary at which the load ΔL was measured. The trends, shown by this study for both the stall regime and the shock regime, are presented in the four parts of figure 14.

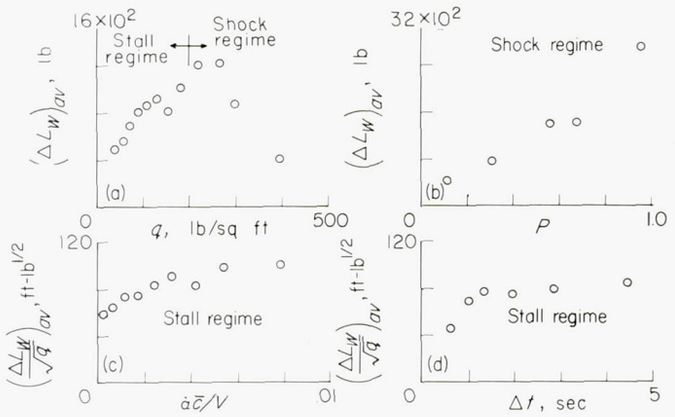

(a) Variation with dynamic pressure.

(b) Variation with penetration.

(c) Variation with abruptness of stall entry.

(d) Variation with time in buffeting.

FIGURE 14.—Trends in wing buffeting loads as shown by method of averages.

Load trends in stall regime.—Stall buffeting in the present study occurs at Mach numbers below a value estimated as 0.65 ± 0.01. All runs in table III (a), therefore, for which $M_B < 0.64$ and for which values of $\dot{\alpha}\bar{c}/V$ and Δt could be established were included in the stall analysis. For each of the 91 runs thus available, the wing-load value ΔL_W and the tail-load value ΔL_T were used, together with the mean of the dynamic-pressure values, tables III (b) and III (c).

The average variation of wing load with q is shown in figure 14 (a). For this plot, the values of ΔL_W were grouped into eight classes, according to the value of q; the plotted variable $(\Delta L_W)_{av}$ is the average of the loads ΔL_W in each class. For the stall regime, the dynamic pressure increases by roughly a factor of 4 (i. e., 42 to 180 lb/sq ft) while the average load increases by a factor of only 2 (i. e., 500 to 1,000 pounds), an increase which is roughly proportional to the square root of q. The dynamic pressure is thus revealed as a major parameter in stalls, but the relation to load appears to be $\Delta L_W \propto \sqrt{q}$ rather than $\Delta L_W \propto q$. This proportionality is used to examine the variation of wing loads in stalls with maneuver abruptness and with time spent in buffeting in figures 14 (c) and 14 (d), respectively, where plots of $(\Delta L_W/\sqrt{q})_{av}$ against $\dot{\alpha}\bar{c}/V$ and Δt are shown. An alleviating effect on load associated with a gradual stall entry is indicated since, at $\dot{\alpha}\bar{c}/V \approx 0$, the loads (expressed as $\Delta L_W/\sqrt{q}$) are as much as 40 percent less than the loads measured in more abrupt maneuvers where $\dot{\alpha}\bar{c}/V \approx 0.008$ radian per chord. The alleviation is indicated in figure 14 (c) to be somewhat exponential in character. With regard to time spent in buffeting, figure 14 (d) suggests that on the average the maximum load encountered during buffeting increases with the total duration of time Δt spent in buffeting. From periods of less than 1 second to periods of 4 to 5 seconds, the increase is of the order of 90 percent but does not appear to be linear.

The trends shown qualitatively in figures 14 (a), 14 (c), and 14 (d) suggest a number of equations which can be written relating wing load to various combinations of the variables representing speed, altitude, time, maneuver abruptness, and structural frequencies. The following equations were among those investigated for the wing loads in stalls:

$$\Delta L_W = a_1 \tag{1}$$

$$\Delta L_W = a_2 q \tag{2}$$

$$\Delta L_W = a_3 \sqrt{q} \tag{3}$$

$$\Delta L_W = a_4 \sqrt{q \log_e (f_n \, \Delta t)} \tag{4}$$

$$\Delta L_W = (a_5 + b_5 e^{-\dot{\alpha}\bar{c}/0.004V}) \sqrt{q} \tag{5}$$

$$\Delta L_W = (a_6 + b_6 e^{-\dot{\alpha}\bar{c}/0.004V}) \sqrt{q \log_e (f_n \, \Delta t)} \tag{6}$$

The values of the arbitrary constants in equations (1) to (6) can be obtained by fitting the equations to the experimental data. An advantage of the least-squares method of fitting lies in the ready availability of precision measures for the constants and of the standard error of estimate of the equation. (For convenient reference, definitions of terms and a summary of least-squares procedures as used in the present investigation are included in appendix A.) The results of the least-squares analysis of the wing loads in stalls are given in table V which shows the equations, the sums of the squares of the residuals, and the standard errors of estimate of the equations, together with the numerical values of the constants and their standard errors of estimate.

Equation (1) is of chief interest for comparison purposes. The value $a_1 = 749$ pounds in table V is the mean of the 91 values of ΔL_W being analyzed. The standard error of estimate, 255 pounds, is in a sense a measure of the error involved

TABLE V.—SUMMARY OF WING-LOAD ANALYSIS IN STALL REGIME

Equation number	Equation	Sum of squares of residuals, $\Sigma\epsilon^2$	Standard error of estimate, s, lb
(1)	$\Delta L_W = a_1$	585×10^4	255
(2)	$\Delta L_W = a_2 q$	770	293
(3)	$\Delta L_W = a_3 \sqrt{q}$	461	226
(4)	$\Delta L_W = a_4 \sqrt{q \log_e (11.7 \, \Delta t)}$	386	206
(5)	$\Delta L_W = (a_5 + b_5 e^{-\dot{\alpha}\bar{c}/0.004V}) \sqrt{q}$	341	196
(6)	$\Delta L_W = (a_6 + b_6 e^{-\dot{\alpha}\bar{c}/0.004V}) \sqrt{q \log_e (11.7 \, \Delta t)}$	287	178

Constants

$a_1 = 749 \pm 27$

$a_2 = 6.54 \pm 0.27$

$a_3 = 74.4 \pm 2.4$

$a_4 = 44.4 \pm 1.3$

$a_5 = 111.5 \pm 6.9$ $\quad b_5 = -55.1 \pm 9.9$

$a_6 = 65.6 \pm 3.8$ $\quad b_6 = -31.6 \pm 5.4$

in the simple assumption that the data on the wing buffeting loads in stalls can be represented by this mean value.

Equations (2) and (3) represent the combined effect of speed and altitude. Equation (2) is analogous to the dimensionless coefficient $C_B=\frac{\Delta L}{qS}$ which parallels the usual coefficients for steady aerodynamic forces and which has been much used in buffeting studies. Equation (3), which was proposed in reference 5 and which also follows from the analysis in appendix B, represents the combined effect of an aerodynamic excitation and an aerodynamic damping. The standard errors of estimate for these equations, 293 pounds and 226 pounds, appear to indicate that q is not as good an indicator of the size of the load as is the mean value, whereas $\sqrt{q}$ is better than the mean. A dependency of load on the square root of the dynamic pressure is also in line with the indications of figure 14 (a) for stalls. Superiority of the square root of the dynamic pressure (as a measure of buffeting) as compared with the first power indicates that in stalls at a given altitude the loads would be directly proportional to the Mach number or the true airspeed, whereas at a given Mach number (or airspeed) the loads would vary directly as the square root of the atmospheric pressure (or density). The linear trend with Mach number revealed by the least-squares analysis is recognizable in the data of figure 7 for stalls when, as for example in figure 7 (a), enough runs are available to give a representative distribution of the time spent in buffeting and the abruptness of the stall entry. The trend with pressure at a given Mach number is less evident, but, for a pressure change from 628 lb/sq ft at 30,000 feet to 1,455 lb/sq ft at 10,000 feet, the corresponding load increase is clearly less than the ratio of the pressures (2.32) and more nearly the square root of the pressure ratio (1.52).

With regard to equation (4) in table V, it would ordinarily be expected that, for a process in which random factors play a part, the probability of occurrence of a given value is higher for a large sample than for a small one. The indication in figure 14 (d) that larger loads are encountered in stalls of longer duration is qualitative confirmation of this expectation. For a stationary random process, as outlined in appendix B, analytical results are available for determining the probability that a given peak value will occur once in a time Δt. These results lead to equation (4), and the standard error of estimate, 206 pounds, represents an improvement over equation (3). In determining the value of a_4, the value of the frequency of wing fundamental bending (11.7 cps, table II) was used for f_n. This frequency is the one most often observed in the wing-shear strain-gage records.

The roughly exponential trend of the variation of $(\Delta L_W/\sqrt{q})_{av}$ with $\dot{\alpha}\bar{c}/V$ indicated in figure 14 (c) suggested the form $be^{-\dot{\alpha}\bar{c}/V\times\text{Constant}}$ as a measure of the effect of maneuver abruptness on the loads in stalls. This form is purely empirical and was adopted simply to account in an approximate way for the observed trend in the data. Although a value of the exponential constant could have been determined by nonlinear regression methods, reference 6, the iterations required make the determination much more laborious than the evaluation of the constants of the linear variations. Preliminary investigations having indicated a value of approximately 0.004 for the constant, this value was used in equations (5) and (6). In comparing equation (5) with equation (3) or equation (6) with equation (4), the relative magnitudes of the standard errors of estimate indicate a significant improvement resulting from inclusion of a measure of the maneuver abruptness. The relative values of a_6 and b_6 (that is, 65.6 and -31.6) indicate that a load alleviation of about 50 percent could be obtained by a gradual stall entry. Although the physical basis for this alleviation is not understood, it may be associated with a less completely developed stall in the slower maneuvers resulting from a less abrupt flow breakdown. A brief study of the correlation between the duration and abruptness of the maneuvers included in the analysis indicates that the larger loads in abrupt maneuvers were not explainable on the basis of stalls of longer duration, but the magnitude of the effect of abruptness indicates that this factor warrants further examination and should not be ignored in other studies of wing buffeting loads in stalls.

The following equations were examined and included in the analysis of the tail loads in stalls:

$$\Delta L_T=A_7 \tag{7}$$

$$\Delta L_T=A_8 q \tag{8}$$

$$\Delta L_T=A_9\sqrt{q} \tag{9}$$

$$\Delta L_T=A_{10}\sqrt{q\log_e(f_n\,\Delta t)} \tag{10}$$

$$\Delta L_T=(A_{11}+B_{11}e^{-\dot{\alpha}\bar{c}/0.004V})\sqrt{q} \tag{11}$$

$$\Delta L_T=(A_{12}+B_{12}e^{-\dot{\alpha}\bar{c}/0.004V})\sqrt{q\log_e(f_n\,\Delta t)} \tag{12}$$

The results of the least-squares analysis shown in table VI are for the same 91 maneuvers used in the wing-loads study. The form of equations (7) to (12) parallels the form of the equations used in the wing-loads study. Because of the

TABLE VI.—SUMMARY OF TAIL-LOAD ANALYSIS IN STALL REGIME

Equation number	Equation	Sum of squares of residuals, $\Sigma\epsilon^2$	Standard error of estimate, s, lb
(7)	$\Delta L_T=A_7$	304×10^4	184
(8)	$\Delta L_T=A_8 q$	384	207
(9)	$\Delta L_T=A_9\sqrt{q}$	280	176
(10)	$\Delta L_T=A_{10}\sqrt{q\log_e(11.7\,\Delta t)}$	257	170
(11)	$\Delta L_T=(A_{11}+B_{11}e^{-\dot{\alpha}\bar{c}/0.004V})\sqrt{q}$	174	140
(12)	$\Delta L_T=(A_{12}+B_{12}e^{-\dot{\alpha}\bar{c}/0.004V})\sqrt{q\log_e(11.7\,\Delta t)}$	161	135

Constants

$A_7=414\pm19$

$A_8=3.59\pm0.19$

$A_9=41.0\pm1.8$

$A_{10}=24.4\pm1.0$

$A_{11}=75.4\pm3.5$ $\quad B_{11}=-51.2\pm5.0$

$A_{12}=44.1\pm2.9$ $\quad B_{12}=-29.2\pm4.1$

empirical nature of the abruptness alleviation expressed by the term $e^{-\dot{\alpha}\bar{c}/0.004V}$, the wing chord and the constant 0.004 were retained in the tail-load calculations. The wing natural frequency was also retained in the expression $\log_e(f_n \Delta t)$.

Comparison of the standard errors of estimate of the equations of table VI indicates the pertinence of the square root of the dynamic pressure, the duration of the stall, and the abruptness of the maneuver. The load alleviation obtainable by a gradual stall entry appears to be even greater than in the case of the wing loads.

Load trends in shock regime.—Buffeting at the Mach numbers of the shock regime was, for the present airplane, encountered under transient conditions in diving turns and pull-ups. In some instances so much speed was lost during a maneuver that buffeting originally encountered at a Mach number of 0.7 ended at Mach numbers of 0.62 or 0.63 with a typical stall recovery. In order to assure a homogeneous class of data, the 26 runs selected as representative of the shock regime were those in which the maximum buffeting load was encountered at Mach numbers above 0.68, as shown by the Mach numbers of tables III (b) and III (c). A plot of values of $(\Delta L_W)_{av}$ against q for these maneuvers, figure 14 (a), appears to indicate a different trend with dynamic pressure in the shock regime than in the stall regime. One reason for the apparent trend with q is found in an examination of the variation of load with penetration beyond the buffet boundary. At a given Mach number, increasing penetration beyond the buffet boundary results in increased amplitude of load fluctuation, but the rate of increase of load with penetration varies with Mach number. These trends for the wing loads in the shock regime are illustrated in figure 15.

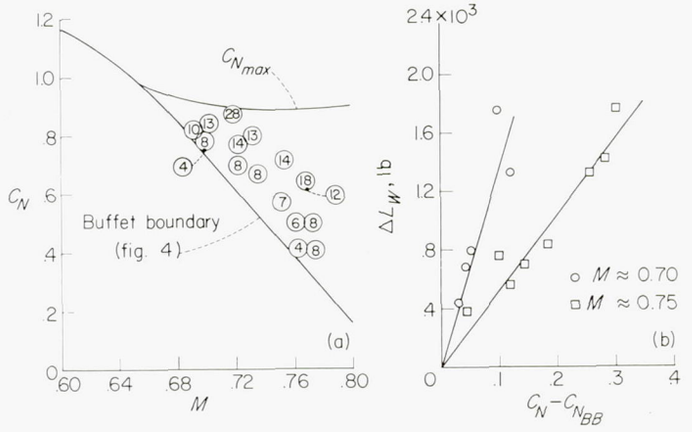

(a) Loads in relation to buffet boundary. (b) Variation of load with penetration

FIGURE 15.—Relationship between buffeting load, C_N, and Mach number.

Figure 15(a) shows the wing-load values ΔL_W plotted on a diagram of the variation of C_N with Mach number. In each symbol is a numeral, indicating the value of ΔL_W in hundreds of pounds. Also shown is the buffet boundary for the shock regime from figure 4. In general, smaller loads occur near the buffet boundary and larger loads, at values of C_N farther removed from the boundary. Figure 15(b) is a plot of load against the difference $\Delta C_N = C_N - C_{N_{BB}}$ for Mach numbers of approximately 0.7 and 0.75. The linear dependence of load on ΔC_N is evident, but the slope $d\Delta L_W/d\Delta C_N$ decreases as M increases.

Shown also in figure 15(a) is a line marked $C_{N_{max}}$. This curve of maximum normal-force coefficient was estimated from a study of recent wind-tunnel data on $C_{N_{max}}$ since specific data for the North American F–51D are not available. If the penetration beyond the buffet boundary at each Mach number is expressed as a ratio denoted by P where

$$P = \frac{C_N - C_{N_{BB}}}{C_{N_{max}} - C_{N_{BB}}} \tag{13}$$

the Mach number dependence of the slopes in figure 15(b) is accounted for. A plot of $(\Delta L_W)_{av}$ against P is shown in figure 14(b). The variation of $(\Delta L_W)_{av}$ with P appears to be linear for the range of flight-test data available; the strong dependence on P effectively masks any dependence on q in figure 14(a).

The equations investigated for wing loads in the shock regime were

$$\Delta L_W = a_{14} \tag{14}$$

$$\Delta L_W = a_{15} q \tag{15}$$

$$\Delta L_W = a_{16} \sqrt{q} \tag{16}$$

$$\Delta L_W = a_{17} P \tag{17}$$

$$\Delta L_W = a_{18} P q \tag{18}$$

$$\Delta L_W = a_{19} P \sqrt{q} \tag{19}$$

The results of the least-squares analysis are given in table VII.

TABLE VII.—SUMMARY OF WING-LOAD ANALYSIS IN SHOCK REGIME

Equation number	Equation	Sum of squares of residuals, $\Sigma\epsilon^2$	Standard error of estimate, s, lb
(14)	$\Delta L_W = a_{14}$	834×10^4	578
(15)	$\Delta L_W = a_{15} q$	1,224	715
(16)	$\Delta L_W = a_{16} \sqrt{q}$	1,009	648
(17)	$\Delta L_W = a_{17} P$	133	238
(18)	$\Delta L_W = a_{18} P q$	192	283
(19)	$\Delta L_W = a_{19} P \sqrt{q}$	125	228

Constants

$a_{14} = 940 \pm 116$

$a_{15} = 2.81 \pm 0.28$

$a_{16} = 52.2 \pm 7.3$

$a_{17} = 2500 \pm 107$

$a_{18} = 9.68 \pm 0.51$

$a_{19} = 153.5 \pm 6.4$

For the tail loads in the shock regime, the equations investigated were similar to those for the wing loads, that is,

$$\Delta L_T = A_{20} \tag{20}$$

$$\Delta L_T = A_{21} q \tag{21}$$

$$\Delta L_T = A_{22} \sqrt{q} \tag{22}$$

$$\Delta L_T = A_{23} P \tag{23}$$

$$\Delta L_T = A_{24} P q \tag{24}$$

$$\Delta L_T = A_{25} P \sqrt{q} \tag{25}$$

The results of the least-squares treatment are shown in table VIII.

TABLE VIII.—SUMMARY OF TAIL-LOAD ANALYSIS IN SHOCK REGIME

Equation number	Equation	Sum of squares of residuals, $\Sigma\epsilon^2$	Standard error of estimate, s, lb
(20)	$\Delta L_T = A_{20}$	218×10^4	295
(21)	$\Delta L_T = A_{21} q$	334	365
(22)	$\Delta L_T = A_{22}\sqrt{q}$	270	335
(23)	$\Delta L_T = A_{23} P$	67	167
(24)	$\Delta L_T = A_{24} Pq$	71	173
(25)	$\Delta L_T = A_{25} P\sqrt{q}$	73	174

Constants

$A_{20} = 508 \pm 59$

$A_{21} = 1.52 \pm 0.24$

$A_{22} = 28.2 \pm 3.8$

$A_{23} = 1254 \pm 76$

$A_{24} = 4.59 \pm 0.28$

$A_{25} = 75.2 \pm 4.6$

For both wing loads and tail loads in the shock regime, the values of the standard errors of estimate show that neither q nor $\sqrt{q}$ is as good a measure of the load as the average value, although $\sqrt{q}$ is somewhat better than q. Inclusion of the penetration in the analysis through the parameter P (eqs. (17), (18), (19), (23), (24), and (25)) results in values of the standard error of estimate which are clearly very much lower than the values for the means (eqs. (14) and (20)). Between equations involving P, Pq, and $P\sqrt{q}$, the indications are not so clear. For wings, equation (19), $\Delta L_W = a_{19} P\sqrt{q}$ has the smallest standard error of estimate, whereas for tail loads equation (23), $\Delta L_T = A_{23} P$ has the smallest standard error of estimate. The lack of a clear indication of the effect of q in the shock regime may be in part the result of the relatively small number of points and the limited range of altitudes that are available at a given Mach number. Another contributing factor may lie in the random character of the buffeting process as discussed in appendix B. The strong dependence of resultant loads on penetration, coupled with the transient character of the maneuvers at speeds above the maximum speed in level flight, would require a more detailed analysis including perhaps not only the extent of penetration but also the length of time spent at or near any given value of penetration. Since the standard errors of estimate for equations (23), (24), and (25) are so nearly the same, it will be assumed that the variable $P\sqrt{q}$ is also applicable to the tail loads in the shock regime.

LOAD EQUATIONS OF BEST FIT

Wing loads.—The summary of the regression analysis of the wing loads measured in the present tests, tables V and VII, indicates that the best fit is obtained with equations (6) and (19). These equations may be written in terms of the values of the regression coefficients as, for the stall regime,

$$\Delta L_W = [65.6 \pm 3.8 - (31.6 \pm 5.4) e^{-\dot{\alpha}_c/0.004V}] \sqrt{q \log_e (11.7\, \Delta t)} \tag{26}$$

and, for the shock regime,

$$\Delta L_W = (153.5 \pm 6.4) P\sqrt{q} \tag{27}$$

In figure 16 a comparison is made of the variations of wing load given by equations (26) and (27) with the effects of q, maneuver abruptness, stall duration, and penetration shown

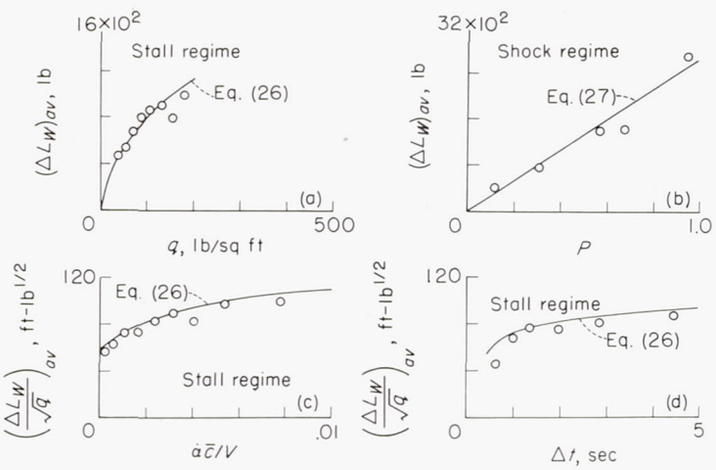

(a) Variation with dynamic pressure. $\overline{\Delta t} = 1.78$ sec; $\left(\overline{\frac{\dot{\alpha}\bar{c}}{V}}\right) = 1.93 \times 10^{-3}$.

(b) Variation with penetration. $\sqrt{\bar{q}} = 17.3$.

(c) Variation with abruptness of stall entry. $\overline{\Delta t} = 1.78$ sec.

(d) Variation with time in buffeting. $\left(\overline{\frac{\dot{\alpha}\bar{c}}{V}}\right) = 1.93 \times 10^{-3}$.

FIGURE 16.—Comparison of results of least-squares analysis with trends shown by method of averages. Circles represent data from figure 14.

in figure 14. The data points of figure 16 are reproduced from figure 14. Shown in each part of the figure are the mean values of the "suppressed" independent variables. For the stall regime, these values $\overline{(\dot{\alpha}\bar{c}/V)} = 0.00193$ radian per chord and $\overline{\Delta t} = 1.78$ seconds have been substituted into equation (26) in order to show in turn the variation of $(\Delta L_W)_{av}$ with q, figure 16 (a), the variation of $(\Delta L_W/\sqrt{q})_{av}$ with $\dot{\alpha}\bar{c}/V$, figure 16 (c), and the variation of $(\Delta L_W/\sqrt{q})_{av}$ with Δt, figure 16 (d). In the shock regime, the average value of q has been substituted into equation (27) to show the trend of $(\Delta L_W)_{av}$ with penetration P. (See fig. 16 (b).)

Since the trend of load with q in the shock regime has been obscured by the large range of values of penetration P, no comparison is shown in figure 16 (a). The agreement between the points representing average trends and the dependency on $\sqrt{q}$ and Δt in equation (26) is substantial and suggests the validity, at least for the present airplane, of the physical concepts represented in the form $\sqrt{q}\log_e(f_n\,\Delta t)$. The exponential character of the alleviation in load obtainable by a gradual stall entry, even though empirical, appears also to represent the trend in the experimental data. Since the effects of duration and abruptness can both be of the order of ± 25 percent of the load for an average condition, the advisability of examining the buffeting of other airplanes on the same basis is indicated.

The expression of the penetration beyond the buffet boundary by means of the ratio $(C_N - C_{N_{BB}})/(C_{N_{max}} - C_{N_{BB}})$ as in equation (13) is purely empirical but, over the range of flight-test data available, appears to give a reasonably good fit to the data (fig. 16 (b)). The linear dependency of load on P assumed in the regression analysis is also empirical, and verification for large penetrations at Mach numbers above 0.70 is not feasible with the present airplane because of operational limits. In particular, it is not known whether the loads for a stall at transonic speeds would be given correctly or whether, as at lower speeds, the abruptness of stall approach would be important; investigation with an airplane with wider operational limits is desirable.

A comparison of the loads calculated by use of equations (26) and (27) with the measured loads on which the numerical values of the regression coefficients are based is shown in figure 17. In each part of figure 17, the line of exact agreement is the solid line with unit slope. The horizontal or vertical distance from any point to this line is the difference between the measured and the calculated load. Parallel to each line of exact agreement are two dashed lines, displaced by the amount of the standard error of estimate. In general, 68 percent of the measured values will vary from the calculated values by less than the amount of the standard error of estimate. The wing loads calculated from equations (26) and (27), when compared with the measured values (figs. 17 (a) and 17 (b)), show generally good agreement. The measured wing loads are estimated to be in error by less

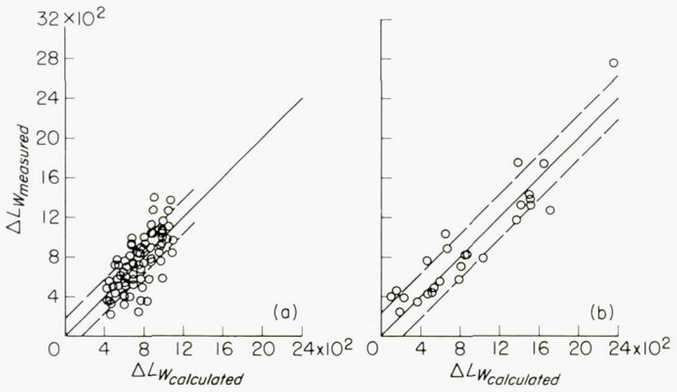

(a) Wing loads, stalls (eq. (26)). (b) Wing loads, shock (eq. (27)).

FIGURE 17.—Comparison of measured and calculated buffeting loads of basic airplane.

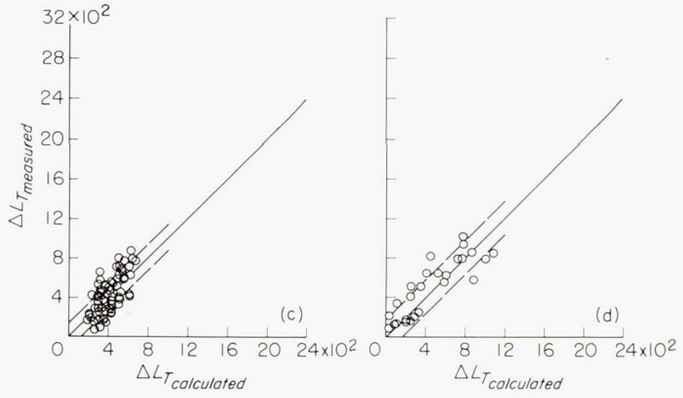

(c) Tail loads, stalls (eq. (28)). (d) Tail loads, shock (eq. (29)).

FIGURE 17.—Concluded.

than ± 130 pounds, as compared with a standard error of estimate for equation (26) of 178 pounds and for equation (27) of 228 pounds. The fact that in the stall regime these two precision measures have roughly the same order of magnitude suggests that, with the present data, regression analysis can probably accomplish little more; in the shock regime, the larger standard error of estimate for equation (27) as compared with the error limits of the experimental data may be a further indication of the need for a more detailed study than has been possible with the present data.

Tail loads.—The summary of the regression analysis of tail loads measured in the present tests indicates that the best fit of the stall data (table VI) is obtained with the equation

$$\Delta L_T = [44.1 \pm 2.9 - (29.2 \pm 4.1)e^{-\dot{\alpha}\bar{c}/0.004V}]\sqrt{q\log_e(11.7\,\Delta t)} \quad (28)$$

whereas the equation which is taken as representing the shock-regime data (table VIII) is

$$\Delta L_T = (75.2 \pm 4.6)P\sqrt{q} \quad (29)$$

Loads calculated from these equations are compared in figures 17 (c) and 17 (d) with the measured loads from which the regression coefficients were obtained. Since equations of the same form as the wing-load equations give such a good fit, the possibility is indicated that the wing is a primary agency in determining tail loads. Since the response of the tail is primarily at a frequency corresponding to that of the fuselage in torsion, the wing may excite the tail through the fuselage. On the other hand, the standard errors of estimate for equation (28), 135 pounds, and for equation (29), 174 pounds, are somewhat larger than the estimated experimental error (± 80 pounds) and this difference, coupled with the correlation coefficient of 0.7 between tail and wing loads, indicates that one or more additional parameters may exist which are important in determining tail loads but which are not disclosed by the present investigation. The propeller slipstream may provide one such agency and the wing wake another, but, since instrumentation suitable for the evaluation of such effects was not incorporated, the relative contributions of the fuselage, the wing wake, and the propeller slipstream cannot be established.

EXTENSION OF RESULTS

Comparison of loads measured on basic and modified airplane.—The large amount of scatter in plots of buffeting load against Mach number in figures 7, 8, 9, and 10 makes difficult any simple determination of the effect of the added wing-tip weights on the magnitude of the buffeting loads. Comparison of figures 7(a) and 9(a), for example, is inconclusive. The equations obtained in the analysis of the buffeting loads on the basic airplane have, therefore, been employed to extend the results obtained on the basic airplane to the analysis of the data for the modified airplane. For the stall regime, equations (26) and (28) have been used, modified only to the extent required to allow for the slightly reduced probability of encountering a given load in a given time since the wing frequency has been reduced. The equations are

$$\Delta L_W=(65.6-31.6e^{-\dot{\alpha}\bar{c}/0.004V})\sqrt{q \log_e (9.3\ \Delta t)} \qquad (30)$$

$$\Delta L_T=(44.1-29.2e^{-\dot{\alpha}\bar{c}/0.004V})\sqrt{q \log_e (9.3\ \Delta t)} \qquad (31)$$

In the shock regime, equations (27) and (29) were used. Values of $\dot{\alpha}\bar{c}/V$ and Δt from table IV(a) were used with average values of q and ΔC_N from tables IV(b) and IV(c) to calculate values of ΔL_W and ΔL_T. These calculated values are compared with the values measured in flight in figure 18,

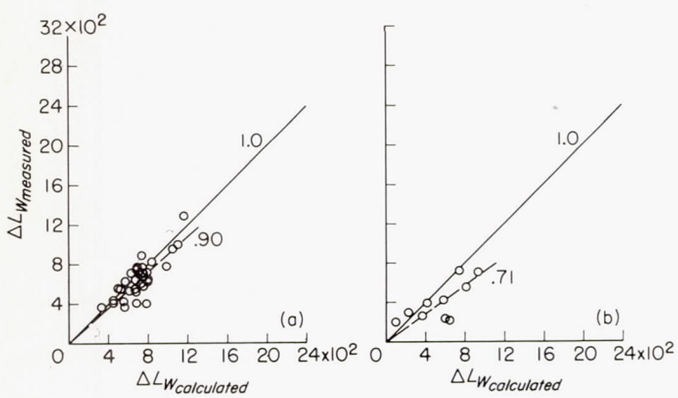

(a) Wing loads, stalls (eq. (30)). (b) Wing loads, shock (eq. (27)).

FIGURE 18.—Effect on loads of a reduction in wing frequency. Buffeting loads measured on modified airplane compared with calculated loads.

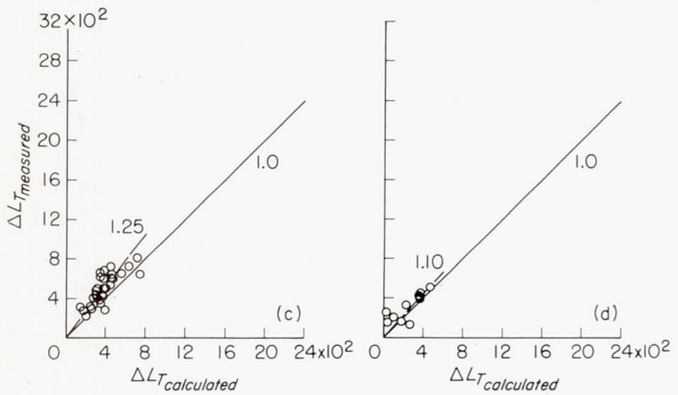

(c) Tail loads, stalls (eq. (31)). (d) Tail loads, shock (eq. (29)).

FIGURE 18.—Concluded.

in which the solid lines are lines of exact agreement. As a measure of the effect of the reduced frequency on load, the average ratio $\frac{(\Delta L)_{modified}}{(\Delta L)_{basic}}$ has been determined, by computing the value of k in the equation

$$(\Delta L)_{modified}=k\ (\Delta L)_{basic} \qquad (32)$$

The values of k for the wing and tail in the stall regime and shock regime, together with their standard errors of estimate, are

$$k_{wing,\ stall}=0.90\pm0.03$$

$$k_{wing,\ shock}=0.71\pm0.07$$

$$k_{tail,\ stall}=1.25\pm0.04$$

$$k_{tail,\ shock}=1.10\pm0.10$$

The dashed straight lines represented by these values of k are shown in figure 18.

For the wing in the stall regime, the value of k indicates an average reduction of 10 ± 3 percent over and above the average reduction of about 4 percent that would be expected because of the reduced probability associated with the frequency reduction. The estimate of a 29 ± 7 percent load reduction in the shock regime is somewhat less reliable than the 10-percent estimate since a smaller number of points is involved, but an overall reduction of something like 15 percent is indicated for the modified airplane.

Comparison of the tail loads measured on the modified airplane with the loads calculated from the least-squares equations as shown in figures 18(c) and 18(d) indicates that the wing modification has increased the tail loads about 15 percent. In buffeting, the motion of the tail is primarily in an antisymmetrical mode at the natural frequency of the tail assembly as restrained in torsion by the fuselage, 9.8 cps in table II. Since the addition of the wing-tip weights reduced the frequency of the wing in fundamental bending from 11.7 to 9.3 cps, table II, wing buffeting of the modified airplane occurs at a frequency only about 0.5 cps removed from the tail buffeting frequency; whereas, with the basic airplane, the difference is nearly 2 cps. The amplitude response of a simple system would be expected to be larger as the frequency of the excitation approaches resonance, and it is possible that a coupling exists between wing and tail vibration modes such that this simple explanation would be sufficient to account for the experimental results. If so, the importance of the fuselage as a coupling agent in the tail-load problem is indicated.

Measured loads compared with results for simplified wing buffeting model.—In appendix B, an equation is developed which gives the form of the relation between pertinent structural and aerodynamic parameters and the mean-square value of the root-structural-shear fluctuations of a stalled wing under the assumption that such buffeting can be treated as the response of a damped linear elastic system to an aerodynamic excitation which is a stationary random process. The buffeting model considered is a simplified wing with one degree of freedom (fundamental bending) and the development parallels, in some respects, the study in refer-

ence 2 of the loads on a tail in a fluctuating airstream. The development is tentative, since the assumption that stall buffeting is a normally distributed stationary random process has yet to be verified, but a comparison of the loads measured in the present study with the tentative relation is of interest.

A primary aerodynamic factor determining the magnitude of the buffeting loads is the power spectrum of the aerodynamic excitation, denoted by the spectrum of the coefficient of section-normal-force fluctuations $c_n^2(\omega)$ in appendix B. Provided that this spectrum possesses certain general dimensional and frequency characteristics (especially a fairly constant level over a band of low frequencies), the details of the shape of the spectrum are of minor concern, but the mean-square value of the excitation $\overline{c_n^2}$ is of great importance. In appendix B, the scale factor in the power spectrum of the excitation is assumed to be the chord, the damping is assumed to be positive and aerodynamic, and the resultant equation for the root-mean-square shear at the root of a wing panel due to buffeting (eq. (B27)) is

$$\sqrt{\overline{L^2}} \approx \frac{1}{2}\left(k\bar{c}S\frac{1-e^{-A/2}}{A/2}\right)^{1/2}\left[\frac{\overline{c_n^2}}{(C_{L_\alpha})_{eff}}\right]^{1/2}\sqrt{q} \tag{33}$$

In this equation the operating conditions of speed and altitude are included in the term $\sqrt{q}$; the geometry of the wing and its stiffness are included in the term in parentheses; whereas the excitation and the aerodynamic damping are represented by the term $\overline{c_n^2}/(C_{L_\alpha})_{eff}$. Little information is available about any spectrum of section normal force, or about the term $(C_{L_\alpha})_{eff}$ which is an effective slope of the lift curve applicable to the aerodynamic damping of small bending oscillations of a stalled wing. Unpublished tests in the Langley 2- by 4-foot flutter research tunnel on a stalled, rigid NACA 65A010 airfoil have given values of $\sqrt{\overline{c_n^2}} \approx 0.07$ over a range of angles of attack beyond the stall. Vibration tests of a similar stalled wing have indicated that over a wide range of reduced frequencies and angles of attack the aerodynamic damping is of the same order of magnitude as that indicated by the two-dimensional slope of the lift curve—that is, $(C_{L_\alpha})_{eff} \approx 2\pi$. Using these two results as a guide to order of magnitude gives a value

$$\left[\frac{\overline{c_n^2}}{(C_{L_\alpha})_{eff}}\right]^{1/2} \approx 0.028 \tag{34}$$

For the present airplane the wing stiffness in a fundamental bending at 11.7 cps is approximately 19,000 pounds per foot. This value for k, together with the dimensions given in table I and the estimate of equation (34), gives the following relation for the root-mean-square buffeting shear at the root of each wing panel:

$$\sqrt{\overline{L^2}} \approx 44\sqrt{q} \tag{35}$$

and for the maximum buffeting shear likely to be encountered in a time Δt (eq. (B33)):

$$\frac{\Delta L_W}{\sqrt{q\log_e(11.7\,\Delta t)}} \approx 62 \tag{36}$$

The least-squares relationship for the wing loads of the present tests with the basic airplane, equation (26), gives as a limit for very abrupt stalls

$$\frac{\Delta L_W}{\sqrt{q\log_e(11.7\,\Delta t)}} = 65.6 \tag{37}$$

whereas for very gradual stalls the limit is

$$\frac{\Delta L_W}{\sqrt{q\log_e(11.7\,\Delta t)}} = 34 \tag{38}$$

and for the data as a whole, equation (4) and table V, an average is

$$\frac{\Delta L_W}{\sqrt{q\log_e(11.7\Delta t)}} = 44.4 \tag{39}$$

The agreement between the constant value 62 of equation (36) and the values 65.6, 34, and 44.4 obtained by least squares (eqs. (37), (38), and (39)) may be fortuitous, in view of the limited knowledge available about buffeting as a stationary random process, the number and character of the assumptions in appendix B, and the limited applicable experimental data on the aerodynamic characteristics of stalled wings. The agreement shown does suggest, however, that further investigation is warranted of both the aerodynamic parameters and their relationship to the buffeting of other airplanes.

Buffeting coefficients.—The results of the present tests indicate that the usual buffeting coefficient of the form $\Delta L/qS$ would, for both wing and tail loads, be overly conservative if coefficients based on loads measurements at high altitudes were used for the estimation of loads at low altitudes. The tests also indicate that, for a given airplane, a simple comparison of loads on the basis of values of the dimensional forms $\Delta L/\sqrt{q}$ or $\Delta L/\sqrt{q\log_e(f_n\,\Delta t)}$ would give more consistent results. To the extent that the simplified analysis of appendix B represents the buffeting of a straight-wing airplane in stalls, a coefficient of the form $\Delta L\Big/\sqrt{qk\bar{c}S(1-e^{-A/2})\log_e(f_n\Delta t)}{A/2}$ would be required to include both the geometry and the elastic properties of the wing, as well as the operating conditions of speed and altitude. Such a coefficient for the present abrupt-stall data would have a value of approximately 0.03. Whether such a coefficient established for one type of airplane would give useful information about another type differing, say, in wing thickness ratio or airfoil section would depend on the aerodynamic characteristics of the wing in stalls, as represented in the term $\overline{c_n^2}/(C_{L_\alpha})_{eff}$. In the absence of more experimental data on a spectrum of aerodynamic excitation for buffeting and on the effects of Mach number and angle of attack on both the spectrum and the aerodynamic damping, a conclusion about a final form of a wing buffeting coefficient cannot be reached. However, should the results for the present unswept-wing airplane be confirmed for other similar airplanes, it should be possible to extend them to swept wings and to tails.

Comparison of wing buffeting loads and design loads.—The results of the least-squares analysis of the wing buffeting loads of the present tests can be used to compare the maximum wing buffeting loads likely to be encountered in stalls with the wing design loads for the North American F–51D airplane. From equation (26) the amplitude of the maximum buffeting-load increment in an abrupt stall of duration Δt is approximately

$$\Delta L_W = 65.6\sqrt{q \log_e(11.7\ \Delta t)} \tag{40}$$

The dynamic pressure of the stall can be expressed in terms of load factor, wing loading, and airplane normal-force coefficient as

$$q = \frac{n\,(W/S)}{C_{N_{BB}}}$$

Therefore ΔL_W can also be expressed as

$$\Delta L_W = 65.6\sqrt{\frac{n\,(W/S)}{C_{N_{BB}}} \log_e\,(11.7\ \Delta t)} \tag{41}$$

The largest value of ΔL_W would be found in stalls at limit load factor at such speed and altitude that $C_{N_{BB}}$ is as small as possible. The least value for $C_{N_{BB}}$ in stalls, figure 4(a), is 1.04. The limit load factor for the test airplane is 7.1 for a gross weight of 9,000 pounds. These values give, for the maximum value of ΔL_W expected,

$$\Delta L_{W_{max}} = 1050\sqrt{\log_e(11.7\ \Delta t)} \tag{42}$$

or, for a stall of 5 seconds' duration, $\Delta L_{W_{max}} = 2{,}650$ pounds.

Such a buffeting load encountered in a stall at limit load factor would be superimposed on a steady wing-panel root structural shear of approximately 22,000 pounds. In terms of a gross weight of 9,000 pounds, a root-shear fluctuation of $\pm 2{,}650$ pounds corresponds to a load-factor fluctuation of approximately ± 0.30.

Fatigue.—For fatigue studies, information is needed on the number of times a given value of load is exceeded in a given period. For a stationary random process, this information is provided by the mean-square load and the power spectrum of the load, as in equation (B26). The simple buffeting model considered in appendix B is a single-degree-of-freedom system which is very lightly damped. For such a system, the response to a random input has the character of a sine wave with a frequency roughly equal to the system natural frequency and an amplitude which fluctuates irregularly. The irregular amplitude fluctuations are characterized by the probability distribution of equation (B31) which gives the number of peaks per second which will exceed a given value. Since the total number of positive peaks per second corresponds to the natural frequency of the system f_n (with an equal number of minimums), equation (B31) provides a simple basis for considering the fatigue aspects of buffeting. (See also ref. 7.) Although based on a simplified model which ignores any contribution of higher vibration modes to the wing buffeting loads, equation (B31) may well represent a satisfactory engineering approximation since modes of frequency higher than first bending ordinarily make but a small contribution to wing-root shear.

CONCLUDING REMARKS

Wing and tail buffeting loads have been measured on a fighter airplane during 194 maneuvers. The half-amplitude of the largest fluctuation in a structural shear was used as a measure of buffeting intensity in each maneuver. Correlation coefficients of 0.9 were found for loads on the left and right wings and the left and right horizontal stabilizers. Least-squares methods have been used to illustrate certain trends in the data; in these studies the loads in the stall regime were found to follow a pattern which differed from that found in the shock regime.

In the stall regime primary variables affecting the magnitude of the loads were speed and altitude as represented by the dynamic pressure, but the square root of the dynamic pressure was a better measure of the load than was the first power, a result which may be due to the action of aerodynamic damping. The loads measured in maneuvers of long duration were, on the average, larger than those measured in maneuvers of short duration, a result which is in accord with considerations of stationary random processes. As compared with abrupt pull-ups, load alleviation of about 50 percent was obtained by a gradual entry into the stall.

In the shock regime, the primary variable affecting the magnitude of the loads was the extent of the penetration beyond the buffet boundary. The data do not provide a clear indication of a dependency of load on dynamic pressure, a result which may be in part attributable to the operating limitations of the airplane which restricted the range of the investigation in the shock regime; a more detailed investigation appears to be required.

Loads were also measured on a modification of the airplane incorporating internal wing-tip weights which reduced the natural frequency of the wing in fundamental bending from 11.7 to 9.3 cps. Analysis of the measured loads indicated a reduction in wing loads of about 15 percent and a similar percentage increase in the tail loads, as compared with the loads on the basic airplane.

The loads on a simplified wing buffeting model have been examined on the assumption that buffeting is the linear response of an aerodynamically damped elastic system to an aerodynamic excitation which is a stationary random process. The results of the present tests for stalls are sufficiently consistent with the results of the analytical study to suggest the examination of the buffeting of other airplanes on the same basis.

LANGLEY AERONAUTICAL LABORATORY,
NATIONAL ADVISORY COMMITTEE FOR AERONAUTICS,
LANGLEY FIELD, VA., *February 11, 1954.*

APPENDIX A

SUMMARY OF STATISTICAL PROCEDURES

A typical problem in linear regression involving a dependent variable w and, say, two independent variables x and y, which is solved by least-squares methods, is usually represented as finding the unknown coefficients a, b, and c in the equation

$$w=ax+by+c$$

given a set of N values of x and y assumed to be exact, and N corresponding measured values of w denoted by w'. For any set of values of a, b, and c, each measured value w'_i and the corresponding calculated value w_i differ by the residual ϵ_i where

$$\begin{aligned}\epsilon_i &= w'_i - w_i \\ &= w'_i - ax_i - by_i - c\end{aligned}$$

The theory of least squares assumes that the "best" values of a, b, and c are those for which the sum of the squares of the residuals $\sum_{i=1}^{N}\epsilon_i^2$ is a minimum, a condition which is fufilled by the values of a, b, and c in the so-called least-squares normal equations which may be represented in matrix form as

$$\begin{bmatrix} N & \sum x & \sum y \\ \sum x & \sum x^2 & \sum xy \\ \sum y & \sum xy & \sum y^2 \end{bmatrix} \begin{Bmatrix} c \\ a \\ b \end{Bmatrix} = \begin{Bmatrix} \sum \omega' \\ \sum \omega' x \\ \sum \omega' y \end{Bmatrix}$$

where the summation $\sum$ denotes $\sum_{i=1}^{N}$. The resulting plane $ax+by+c$ passes through the point $(\overline{w}',\overline{x},\overline{y})$ determined by the mean values of w', x, and y.

The present report is concerned with the application of least-squares methods to equations of the type where $c=0$, and

$$w=ax$$

or

$$w=ax+by$$

that is, problems where the least-squares line or plane is required to pass through the origin ($w=x=y=0$). In this case for two independent variables, x and y, the values of a and b are given by the normal equations

$$\begin{bmatrix} \sum x^2 & \sum xy \\ \sum xy & \sum y^2 \end{bmatrix} \begin{Bmatrix} a \\ b \end{Bmatrix} = \begin{Bmatrix} \sum w'x \\ \sum w'y \end{Bmatrix}$$

The solution may conveniently be written in terms of the inverse matrix which for second-order matrices is given by

$$\begin{bmatrix} c_{11} & c_{12} \\ c_{21} & c_{22} \end{bmatrix} = \begin{bmatrix} \sum x^2 & \sum xy \\ \sum xy & \sum y^2 \end{bmatrix}^{-1}$$

$$= \frac{1}{\sum x^2 \sum y^2 - (\sum xy)^2} \begin{bmatrix} \sum y^2 & -\sum xy \\ -\sum xy & \sum x^2 \end{bmatrix}$$

Accordingly

$$\begin{Bmatrix} a \\ b \end{Bmatrix} = \begin{bmatrix} c_{11} & c_{12} \\ c_{21} & c_{22} \end{bmatrix} \begin{Bmatrix} \sum w'x \\ \sum w'y \end{Bmatrix}$$

The sum of the squares of the residuals is given by

$$\sum \epsilon^2 = \sum w'^2 - [a \quad b] \begin{Bmatrix} \sum w'x \\ \sum w'y \end{Bmatrix}$$

A measure of the spread in the measured values of w' is $s_{w'}$, the standard error of w' defined by

$$s_{w'} = \sqrt{\frac{\sum (w'-\overline{w}')^2}{N-1}}$$

where $\overline{w}'$ is the arithmetic mean of the measured values $\frac{\sum w'}{N}$. The standard error of w' is usually most easily evaluated by the equation

$$s_{w'} = \sqrt{\frac{N\sum w'^2 - (\sum w')^2}{N(N-1)}}$$

The standard error of the mean $s_{\overline{w}'}$ is proportional to $s_{w'}$ and inversely proportional to the square root of the number of points, that is,

$$s_{\overline{w}'} = \frac{s_{w'}}{\sqrt{N}}$$

A measure of the ability of the regression equation to represent the data is given by the standard error of estimate of the equation, which for $w=ax$ is

$$s_{w_1} = \sqrt{\frac{\sum \epsilon^2}{N-2}}$$

and for $w=ax+by$ is

$$s_{w_2} = \sqrt{\frac{\sum \epsilon^2}{N-3}}$$

The standard errors of estimate of the constants a and b are related to the standard error of estimate of the equation and the terms on the principal diagonal of the inverse of the matrix of the coefficients of the normal equation by the relations

$$s_a = \sqrt{c_{11}}\, s_w$$

$$s_b = \sqrt{c_{22}}\, s_w$$

The standard error of w', that is, $s_{w'}$, is a measure of the error involved in representing the N values of w' by their mean value $\overline{w}'$. An equation, say, $w=ax$, for which the

standard error of estimate s_w is smaller than $s_{w'}$ would ordinarily be considered an improvement over the mean-value representation, since it implies that specification of a value of x gives better information about the value of w' than does the mean value $\overline{w'}$. The methods of the analysis of variance give a statistical estimate of whether the equation $w=ax$ is improved by the addition of another variable y to give $w=a_2x+b_2y$. For this particular question (see ref. 8) if $\sum\epsilon_1^2$ and $\sum\epsilon_2^2$ represent the sum of the squares of the residuals of the one- and two-parameter equations being compared and the ratio

$$F=\frac{\sum\epsilon_1^2-\sum\epsilon_2^2}{s_{w_2}^2}$$

exceeds a certain critical value, then, on the basis of the evidence at hand, the chances are at least 100 to 1 that the improvement is real. The magnitude of the critical value of F depends upon the number of values N. For $N=25$, 50, and 100, the values of F are 7.97, 7.20, and 6.91, respectively.

Although linear dependency between two variables w and x is usually expressed by a relationship of the type $w=ax+c$ when the measured values of x are considered exact, or in any event more nearly under experimental control than the measurements of w, there are instances when a more general measure of the linear dependency of two variables is desired. The coefficient of linear correlation r is such a measure which does not depend on the choice of w or x as independent variable or on the units of w and x. The value of r is usually calculated from the relation

$$r=\frac{N\sum wx-(\sum w)(\sum x)}{\sqrt{[N\sum w^2-(\sum w)^2][N\sum x^2-(\sum x)^2]}}$$

but it can be shown that this value is equal to the square root of the product of the slopes a and a' in the two regression equations

$$w=ax+c$$

and

$$x=a'w+c'$$

that is

$$r=\sqrt{a'a}$$

The values of r fall within the range $-1\leqq 0\leqq 1$, unit values indicating exact linear dependence and zero indicating complete independence of the two variables. A negative correlation coefficient indicates inverse dependency; that is, increasing values of one variable are associated with decreasing values of the other.

For convenience in computation, all of the summations required in regression and correlation studies of the variables w and x may be obtained by expressing the N pairs of related measurements such as $(w,x)_i$ in the rectangular matrix

$$||M||=\begin{Vmatrix} 1 & w_1 & x_1 \\ 1 & w_2 & x_2 \\ \cdot & \cdot & \cdot \\ \cdot & \cdot & \cdot \\ \cdot & \cdot & \cdot \\ 1 & w_N & x_N \end{Vmatrix}$$

and premultiplying this matrix by its transpose $||M^T||$, so that the following symmetrical square matrix results:

$$[M^TM]=\begin{bmatrix} N & \sum w & \sum x \\ \sum w & \sum w^2 & \sum wx \\ \sum x & \sum xw & \sum x^2 \end{bmatrix}$$

Similar considerations apply, of course, to the study of w, x, and y. More detailed treatment of the precision and interpretation of regression studies will be found in references 8 and 9. Numerical procedures are described in references 10 and 11.

APPENDIX B

LOADS ON A SIMPLIFIED WING BUFFETING MODEL

References 2 and 5 have illustrated the application of methods developed in the study of stationary random processes [2] to the problem of the buffeting of an elastic structure such as a tail located in a turbulent airstream. A simple parallel treatment is possible which illustrates the form of the relationship between the airfoil motions and pertinent structural, geometric, and aerodynamic parameters for an elastically restrained airfoil subjected to the excitation of its own separated flow.

The simplified model considered in the present section is a rigid airfoil of mass m, span b, mean chord $\bar{c}$, and area S restrained by a spring of stiffness k to oscillate in vertical motion only. The vertical displacement $z(t)$ from equilibrium can be expressed by the differential equation for a single-degree-of-freedom system:

$$\frac{d^2z}{dt^2}+2\gamma\omega_n\frac{dz}{dt}+\omega_n{}^2z=\frac{F(t)}{m} \tag{B1}$$

where γ is the ratio of the damping to critical damping, ω_n is the undamped natural circular frequency given by the relation

$$\omega_n{}^2=\frac{k}{m} \tag{B2}$$

and $F(t)$ is an impressed force. For an airfoil in a stream of air of dynamic pressure q, the exciting force associated with a time-varying fluctuating section normal-force coefficient $c_n(t)$ would be (three-dimensional effects being ignored)

$$F(t)=c_n(t)\bar{c}bq \tag{B3}$$

If $c_n(t)$ is a random function of time but is expressible in terms of a power spectrum of the coefficient of the section-normal-force fluctuations $c_n{}^2(\omega)$ such that the mean-square section normal-force coefficient is

$$\overline{c_n{}^2}=\int_0^\infty c_n{}^2(\omega)\,d\omega \tag{B4}$$

then $z(t)$ is also a random function of time, expressible by a power spectrum $z^2(\omega)$ and, by reason of equation (B1), $z^2(\omega)$ is related to $c_n{}^2(\omega)$ through the admittance $A^2(\omega)$ of the system by the relation

$$z^2(\omega)=\frac{\bar{c}^2b^2q^2}{m^2\omega_n{}^4}\,c_n{}^2(\omega)A^2(\omega) \tag{B5}$$

where the admittance taken as the square of the amplitude ratio of the system is

$$A^2(\omega)=\frac{1}{\left(1-\dfrac{\omega^2}{\omega_n{}^2}\right)^2+4\gamma^2\dfrac{\omega^2}{\omega_n{}^2}} \tag{B6}$$

[2] Time variations of a quantity during a particular time interval may be studied by the method of Fourier analysis, and this method can be generalized to apply to a continuing nonperiodic disturbance through use of the concept of a stationary random process. This concept applies when the underlying physical mechanism which gives rise to an irregular disturbance does not change in time and the resultant process is thus both stationary and random. As a random process, it can be described by certain statistical parameters (mean, mean square, and power spectrum are ordinarily of chief interest); as a stationary random process, these parameters do not change in time and prediction on a statistical basis is therefore possible. For a more complete discussion see references 12 and 13.

The mean-square displacement of the airfoil is given by the definite integral of equation (B5), that is,

$$\overline{z^2}=\frac{\bar{c}^2b^2q^2}{m^2\omega_n{}^4}\int_0^\infty c_n{}^2(\omega)A^2(\omega)\,d\omega \tag{B7}$$

Evaluation of the integral in equation (B7) could be a complex problem, even under the assumption of positive damping, but, for small values of the damping, the admittance $A^2(\omega)$ in equation (B7) changes very rapidly in the frequency band in the vicinity of resonance, $\omega=\omega_n$, and it is possible to substitute for $c_n{}^2(\omega)$ in equation (B7) its value at ω_n and to write the approximate relation

$$\overline{z^2}\approx\frac{\bar{c}^2b^2q^2}{m^2\omega_n{}^4}\,c_n{}^2(\omega_n)\int_0^\infty A^2(\omega)\,d\omega \tag{B8}$$

For the admittance given by equation (B6), the area under the admittance curve is inversely proportional to the damping ratio since

$$\int_0^\infty A^2(\omega)\,d\omega=\frac{\pi\omega_n}{4\gamma} \tag{B9}$$

Therefore, the mean-square displacement is

$$\overline{z^2}\approx\frac{\pi\bar{c}^2b^2q^2}{4\gamma m^2\omega_n{}^3}\,c_n{}^2(\omega_n) \tag{B10}$$

For the simplified buffeting model considered, aerodynamic damping forces would originate in the velocity of the vertical motion $\dot{z}$ and the damping ratio could be expressed as

$$\gamma=\frac{q\bar{c}b}{2m\omega_nV}\,(C_{L_\alpha})_{eff} \tag{B11}$$

where $(C_{L_\alpha})_{eff}$ will be considered as an effective slope of the lift curve applicable to the damping of small bending motions of a stalled airfoil. The present flight tests have been concerned with values of wing root shear, which are analogous not to the airfoil displacement but to the load $L=kz$ exerted on the spring support. Hence, an expression for the mean-square shear load in buffeting obtained from equations (B2), (B10), and (B11) would be $\overline{L^2}=k^2\overline{z^2}$ or

$$\overline{L^2}\approx\frac{\pi k\bar{c}bqV}{2(C_{L_\alpha})_{eff}}\,c_n{}^2(\omega_n) \tag{B12}$$

Two characteristics pertinent to the definition of the spectrum $c_n{}^2(\omega)$ are its level, as determined by the mean square, and its shape, or the frequency distribution of the excitation. These characteristics may be expressed by writing $c_n{}^2(\omega)$ in the form

$$c_n{}^2(\omega)=\overline{c_n{}^2}\Phi(\omega) \tag{B13}$$

where $\Phi(\omega)$ is the power-spectral-density function or shape parameter which defines the contribution to $\overline{c_n{}^2}$ from the

excitation in any frequency band between ω and $\omega+d\omega$. Thus, in view of equation (B4),

$$\int_0^\infty \Phi(\omega)\,d\omega=1 \tag{B14}$$

For a section property, it seems probable that the frequency ω is a less fundamental variable for defining the shape of the spectrum than a reduced frequency based on the speed V and a linear dimension related to the size of the airfoil or the chordwise extent of separation. For the chord as the pertinent linear dimension, a reduced shape parameter $\Phi\left(\frac{c\omega}{V}\right)$ is related to $\Phi(\omega)$ by requirements of dimensional consistency, that is

$$\Phi(\omega)=\frac{c}{KV}\Phi\left(\frac{c\omega}{V}\right) \tag{B15}$$

where the constant K which appears in the denominator is the area under the curve defined by the reduced shape parameter. Thus, on the basis of dimensional considerations, the spectrum $c_n^2(\omega)$ may be written as

$$c_n^2(\omega)=\overline{c_n^2}\,\frac{c}{KV}\Phi\left(\frac{c\omega}{V}\right) \tag{B16}$$

where

$$K=\int_0^\infty \Phi\left(\frac{c\omega}{V}\right)d\left(\frac{c\omega}{V}\right) \tag{B17}$$

and the intensity of the fluctuations of section normal force at a particular frequency is seen to depend not only on the mean-square value $\overline{c_n^2}$ but also on the scale and speed and on the spectral distribution of the excitation as expressed by the reduced shape parameter. From equation (B16), which provides a value for $c_n^2(\omega_n)$, the mean-square buffeting load is

$$\overline{L^2}\approx\frac{\pi k\bar{c}^2bq}{2K(C_{L_\alpha})_{eff}}\,\overline{c_n^2}\,\Phi\left(\frac{c\omega_n}{V}\right) \tag{B18}$$

Little information is available concerning the shape parameter $\Phi\left(\frac{c\omega}{V}\right)$ for stalled airfoils. In references 2 and 14, isotropic turbulence has been used to illustrate a random excitation expressible by a power spectrum. At a point in isotropic turbulence, the turbulent component of velocity $w(t)$ normal to the free-stream velocity V results in an equivalent fluctuating angle of attack $\alpha(t)=\frac{w(t)}{V}$ which has a mean-square value $\overline{\alpha^2}$ and a spectrum $\alpha^2(\omega)$ that can be written in terms of a reduced frequency $l\omega/V$ as

$$\alpha^2(\omega)=\overline{\alpha^2}\,\frac{l}{KV}\Phi\left(\frac{l\omega}{V}\right) \tag{B19}$$

where l is a linear dimension characteristic of the scale of the turbulence, and

$$\Phi\left(\frac{l\omega}{V}\right)=\frac{1+\frac{3l^2\omega^2}{V^2}}{\left(1+\frac{l^2\omega^2}{V^2}\right)^2} \tag{B20}$$

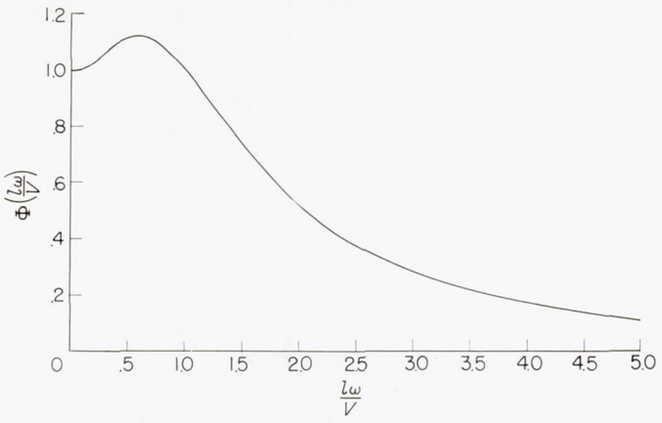

FIGURE 19.—Shape of spectral distribution function (eq. (B20)).

for which the constant K of equation (B17) is equal to π. This particular shape parameter, which has been plotted in figure 19, is relatively constant and close to unity for values of reduced frequency less than 1 and then falls rapidly to low values. The assumption that the spectrum of the coefficient of the section-normal-force fluctuations on a stalled airfoil $\Phi\left(\frac{c\omega}{V}\right)$ has a shape similar to that expressed in equation (B20) with $l=c$ leads to an estimate of π for the constant K in equation (B18) and provides a guide for estimating the value of $\Phi\left(\frac{\bar{c}\omega_n}{V}\right)$.

In equation (B3) and thus in equation (B18), section properties have been applied to the excitation of the entire wing, an application which, in general, would be expected to overestimate the net excitation since fluctuations at one chord station would not necessarily be in phase with fluctuations at another station. A simple overall correction is possible, however, which is based on a correlation function observed in isotropic turbulence and is directly related to the spectrum, equation (B19). This correction is similar to the length correction used in hot-wire anemometry and is used in reference 14 to relate the mean-square angle-of-attack fluctuation at a point along the span to the mean-square value over the entire span. It involves the ratio of the scale of the turbulence to the span b. If the same overall correction is applied to the coefficient of section-normal-force fluctuations to take care of the major effects of spanwise load correlation, the wing $\overline{C_N^2}$ would be related to the section $\overline{c_n^2}$ by the equation

$$\overline{C_N^2}=\overline{c_n^2}\,\frac{\bar{c}}{b}\,(1-e^{-b/\bar{c}}) \tag{B21}$$

This same overall correction leads to the final expression, applicable to the simplified model, for $\overline{L^2}$ the mean-square force exerted on the model support

$$\overline{L^2}\approx\frac{k\bar{c}^2bq}{2}\,\frac{1-e^{-b/\bar{c}}}{b/\bar{c}}\,\frac{\overline{c_n^2}}{(C_{L_\alpha})_{eff}}\,\Phi\left(\frac{\bar{c}\omega_n}{V}\right) \tag{B22}$$

With slight modification, an expression applicable to the root shear of a wing panel can be obtained from equation (B22). For wing motions which are simplified in that only

fundamental bending at natural frequency ω_n is considered, the vertical motion varies along the semispan direction y in accordance with the shape of the bending mode $z_1(y)$ (taken as unity at the tip). The stiffness k would be an effective stiffness corresponding to this mode, where

$$k=m_e\omega_n^2 \tag{B23}$$

and m_e is an effective mass for bending in this mode, given by the integral of the product of the spanwise wing mass distribution $m(y)$ and the square of the mode shape, or

$$m_e=\int_0^{b/2} m(y)z_1^2(y)\,dy \tag{B24}$$

Thus for the assumed wing, the mean-square root buffeting shear for one wing panel of span $b/2$ would be

$$\overline{L^2}\approx\frac{k\bar{c}^2qb}{4}\,\frac{1-e^{-b/2\bar{c}}}{b/2\bar{c}}\,\frac{\overline{c_n^2}}{(C_{L_\alpha})_{eff}}\,\Phi\left(\frac{\bar{c}\omega_n}{V}\right) \tag{B25}$$

or, in terms of aspect ratio $A=\frac{b}{\bar{c}}$ and total wing area $S=b\bar{c}$, the mean-square root shear would be

$$\overline{L^2}\approx\frac{k\bar{c}Sq}{4}\,\frac{1-e^{-A/2}}{A/2}\,\frac{\overline{c_n^2}}{(C_{L_\alpha})_{eff}}\,\Phi\left(\frac{\bar{c}\omega_n}{V}\right) \tag{B26}$$

For a given structure (c and ω_n fixed) the proportionality between $\overline{L^2}$ and q (or V^2) could be modified by changes in the value of the shape parameter $\Phi\left(\frac{\bar{c}\omega_n}{V}\right)$ with speed. If, however, the value of the reduced frequency $\frac{\bar{c}\omega_n}{V}$ lies in a nearly flat portion at the low-frequency end of the spectrum, then, for a spectrum with a shape parameter like that given by equation (B20), the value of the shape parameter $\Phi\left(\frac{\bar{c}\omega_n}{V}\right)$ in equation (B26) can be replaced by its approximate value, unity, and

$$\overline{L^2}\approx\frac{k\bar{c}S}{4}\,\frac{1-e^{-A/2}}{A/2}\,\frac{\overline{c_n^2}}{(C_{L_\alpha})_{eff}}\,q \tag{B27}$$

Such a substitution would be valid over a range of speeds which is wider for low values of $\bar{c}$ and low values of natural frequency ω_n.

The foregoing development deals with the mean-square load on a wing panel. If the buffeting of the simplified model can be considered a normally distributed stationary random process, then the relationship between the mean-square root shear $\overline{L^2}$ and the probable amplitude ΔL of the maximum fluctuation occurring in a time interval Δt is fixed by the power spectrum of the load $L^2(\omega)$. By use of the results obtained in reference 12, the number of peak values per second which will exceed a particular level ΔL_1 can be shown to be (when ΔL_1 is large)

$$N_{\Delta L_1}=\frac{1}{2\pi}\left[\frac{\int_0^\infty \omega^2L^2(\omega)\,d\omega}{\int_0^\infty L^2(\omega)\,d\omega}\right]^{1/2} e^{-\Delta L_1^2/2\overline{L^2}} \tag{B28}$$

Just as equation (B7) was simplified to equation (B8) the term in brackets is easily evaluated, since

$$\frac{\int\omega^2L^2(\omega)\,d\omega}{\int L^2(\omega)\,d\omega}\approx\frac{\int\omega^2A^2(\omega)\,d\omega}{\int A^2(\omega)\,d\omega} \tag{B29}$$

and, for an admittance given by equation (B6),

$$\int_0^\infty \omega^2A^2(\omega)\,d\omega=\omega_n^2\int_0^\infty A^2(\omega)\,d\omega \tag{B30}$$

Therefore, since $\omega_n=2\pi f_n$,

$$N_{\Delta L_1}=f_ne^{-\Delta L_1^2/2\overline{L^2}} \tag{B31}$$

and a value of ΔL will, on the average, be exceeded once in a time interval Δt given by the expression

$$\frac{1}{\Delta t}=f_ne^{-\Delta L^2/2\overline{L^2}} \tag{B32}$$

or the value ΔL which occurs once, on the average, in a time interval Δt is given by the equation

$$\Delta I=\sqrt{2\overline{L^2}\log_e(f_n\,\Delta t)} \tag{B33}$$

The ratio $\Delta L/\sqrt{\overline{L^2}}$ is plotted in figure 20 for two values of f_n, 9.3 and 11.7 cps, corresponding to the basic and modified wing in the fundamental bending mode, the predominant mode in the wing buffeting time histories observed in the present investigation.

Combination of equations (B27) and (B33) leads to an equation which relates the maximum load ΔL_W (as measured in the present tests) in a stall of duration Δt to the geometric, structural, and aerodynamic characteristics of the simplified wing,

$$\Delta L_W\approx\left(\frac{k\bar{c}S}{2}\,\frac{1-e^{-A/2}}{A/2}\right)^{1/2}\sqrt{\frac{\overline{c_n^2}}{(C_{L_\alpha})_{eff}}}\,\sqrt{q\log_e(f_n\,\Delta t)} \tag{B34}$$

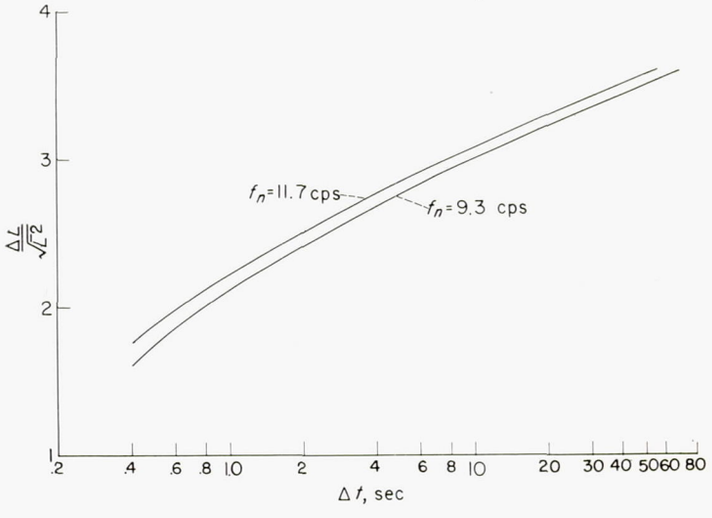

FIGURE 20.—Variation of maximum-expected buffeting load with time spent in buffeting and wing natural frequency (eq. (B33)).

REFERENCES

1. Stokke, Allen R., and Aiken, William S., Jr.: Flight Measurements of Buffeting Tail Loads. NACA TN 1719, 1948.
2. Liepmann, H. W.: On the Application of Statistical Concepts to the Buffeting Problem. Jour. Aero. Sci., vol. 19, no. 12, Dec. 1952, pp. 793–800, 822.
3. Aiken, William S., Jr.: Flight Determination of Wing and Tail Loads on a Fighter-Type Airplane by Means of Strain-Gage Measurements. NACA TN 1729, 1948.
4. Skopinski, T. H., Aiken, William S., Jr., and Huston, Wilber B.: Calibration of Strain-Gage Installations in Aircraft Structures for the Measurement of Flight Loads. NACA Rep. 1178, 1954. (Supersedes NACA TN 2993.)
5. Liepmann, H. W.: Parameters for Use in Buffeting Flight Tests. Rep. No. SM–14631, Douglas Aircraft Co., Inc., Jan. 3, 1953.
6. Scarborough, James B.: Numerical Mathematical Analysis. The Johns Hopkins Press (Baltimore), 1930.
7. Miles, John W.: An Approach to the Buffeting of Aircraft Structures by Jets. Rep. No. SM–14795, Douglas Aircraft Co., Inc., June 1953.
8. Goulden, C. H.: Methods of Statistical Analysis. John Wiley & Sons, Inc., c.1939.
9. Anderson, R. L., and Bancroft, T. A.: Statistical Theory in Research. McGraw-Hill Book Co, Inc., 1952.
10. Dwyer, Paul S.: A Matrix Presentation of Least Squares and Correlation Theory With Matrix Justification of Improved Methods of Solution. Annals of Mathematical Statistics, vol. 15, no. 1, Mar. 1944, pp. 82–89.
11. Dwyer, Paul S.: Linear Computations. John Wiley & Sons, Inc., c. 1951.
12. Rice, S. O.: Mathematical Analysis of Random Noise. Pts. I and II. Bell Syst. Tech. Jour., vol XXIII, no. 3, July 1944, pp. 282–332; Pts. III and IV, vol. XXIV, no. 1, Jan. 1945, pp. 46–156.
13. James, Hubert M., Nichols, Nathaniel B., and Phillips, Ralph S.: Theory of Servomechanisms. McGraw-Hill Book Co., Inc., 1947.
14. Liepmann, H. W.: An Approach to the Buffeting Problem From Turbulence Considerations. Rep. No. SM–13940, Douglas Aircraft Co., Inc., Mar. 13, 1951.

U. S. GOVERNMENT PRINTING OFFICE: 1956